Delft University of Technology
Master's Thesis in Embedded Systems

Sensing human activity with dark light

Hajo Kleingeld

Sensing human activity with dark light

Master's Thesis in Embedded Systems

Embedded Software Section
Faculty of Electrical Engineering, Mathematics and Computer Science
Delft University of Technology
Mekelweg 4, 2628 CD Delft, The Netherlands

Hajo Kleingeld
hajokleingeld@gmail.com

12th December 2017

Author

Hajo Kleingeld (hajokleingeld@gmail.com)

Title

Sensing human activity with dark light

MSc presentation

19th December 2017

Graduation Committee

Prof. dr. K.G. Langendoen (Chair)	Delft University of Technology
dr. M. Zuñiga (Daily Supervisor)	Delft University of Technology
dr. C. Doerr	Delft University of Technology

Abstract

Nowadays, 19% of the global energy consumption is used for lighting. For this reason, saving energy in lighting is vital. A simple way to save energy is to simply turn the lights off, or reduce the amount of light used when nobody is around. This thesis proposes a new method for luminaires to detect the presence of humans and objects which only uses a photodiode and a fraction of the light a luminaire normally emits, namely *Dark Sensing.*

Dark sensing works by sending out short flashes of light. These short flashes use little energy and are barely visible to the user. These flashes get reflected by the environment and received by a photodiode placed next to the light. By extracting a key feature of the received flash, we obtain a metric representing the surrounding area. If an object enters the observed area, the reflections of light will change. These changes will be noticed by the system, which triggers a detection resulting in the light being turned on.

A prototype was created which shows the potential of the newly developed method. The prototype was tested in two different environments and detects between 73% and 90% of bypassing pedestrians, depending on the accepted false positive ratio (0 to 0.05).

Preface

For me, finding a thesis topic was no easy task. All I knew was: "I want to build something cool". So when it was time to select the topic, I decided the best course of action was to visit the professors who gave the most interesting lectures. When I went to visit the Embedded Software Group on the 9th floor of EEMCS and learned about the world of Visible Light Communication (VLC), I knew I found the right topic.

The basic concept of VLC was familiar to me. "It's just really fast morse code", is a sentence I used a lot to explain VLC to my friends. When I noticed that my (non-technical) friends could not grasp this concept, I was sure that I could help create to something innovative and new. With this motivation I started the *Dark Sensing* project.

The Dark Sensing project has learned me a lot the last year. Even though finishing the project took longer than expected and wasn't always a fun activity, I'm happy that im finaly done and am happy with the result. This thesis would not look the same without the help of some persons who need to be thanked. First of all, I need to thank Marco for supervising the project. Even though our opinions where not always aligned, without his guidance the project would not have been this successful. I also need to thank Rens and the rest of the VLC power group for their help for their ideas and general feedback. I also thank my house-mates for their help. Finally I want to thank my friends an family for their support while I was working on my master thesis.

Hajo Kleingeld

Delft, The Netherlands
12th December 2017

Contents

Preface **v**

1 Introduction **1**

1.1 Problem statement 2

1.2 Contributions 2

1.3 Organisation 3

2 Background and related work **5**

2.1 Background 5

2.1.1 Dimming of an LED 5

2.1.2 The Phong model 7

2.2 Related Work 11

2.2.1 Passive localisation 11

2.2.2 Passive Visible Light Localisation 11

2.2.3 Other related projects 14

3 Model **15**

3.1 Model description 15

3.1.1 Model Adjustments 15

3.1.2 Calculation process 16

3.2 Verification 16

3.3 Modelling of the hallway 19

3.4 Modelling of the street 20

3.5 Results 21

3.6 Conclusions 21

4 Platform **25**

4.1 system components 25

4.1.1 Flash generator 25

4.1.2 Reflection receiver 26

4.1.3 Analyser 26

4.2 Implementation 27

4.3 Summary 28

5 Flash Analysis **31**
5.1 Flash properties 32
5.2 Flash features 32
5.2.1 Feature considerations 32
5.2.2 Feature comparison 34
5.3 Flash period 36
5.4 Conclusion 36

6 Analyser **37**
6.1 Received signals 37
6.2 Filter methods 39
6.2.1 Low-pass filters 39
6.2.2 High-pass filters 40
6.2.3 Moving average filters 40
6.2.4 Differential filter 41
6.2.5 Filter overview 42
6.3 Detection threshold 42
6.3.1 Standard deviation based threshold 44
6.4 Conclusion 45

7 System evaluation **47**
7.1 Test set-up 47
7.2 Algorithm parameters 50
7.3 Evaluation 51
7.4 Conclusion 53

8 Conclusions and Future Work **55**
8.1 Conclusions 55
8.2 Future Work 55

A Code repository **59**

B Flash analyser schematics **61**
B.1 LED driver 61

Chapter 1

Introduction

Nowadays, 19% of the global energy consumption is used for lighting. For this reason, saving energy in lighting is vital. A simple way to save energy is to simply turn the lights off, or reduce the amount of light used when nobody is around. This thesis proposes a new method for luminaires to detect the presence of humans and objects, namely *Dark Sensing*.

The idea of human sensing is not new. Everybody in the western world has walked into a room where the lights suddenly turned on once they entered. The most common method to create this effect is to make use of a PIR (passive-infrared) sensor. By monitoring the infra-red radiation (heat) in the area, it can detect changes in the environment and toggle the light based on these changes. This method works very well but has several drawbacks. The first is that it's unable to detect objects with the same surface temperature as the environment, for example a car where the engine has just been turned on. Another drawback is that the PIR method has no potential for communication without the addition of extra components. Dark sensing attempts to overcome these drawbacks by only using a photodiode and the light in the visible spectrum a luminaire normally emits.

This thesis explores the idea of detecting changes in the environment with reflections of visible light. The proposed system works in the following manner: If nothing is in the area, the light will be turned on, but outputting a very low light level. Some of the light will reflect off the environment back to the light source. This can be measured with the photodiode. The signal received is a measure of the illuminated area. If something were to change in that area, a car drives by for example, then the reflections in the environment will change and therefore the light perceived by the photodiode will change as well. These changes will then result in a detection by the system which will turn the light on at full brightness. An overview of the scenario can be seen in 1.1.

The ultimate goal of the proposed system is to reduce the time the light needs to be on the nearly zero. This will lead to a light which barely con-

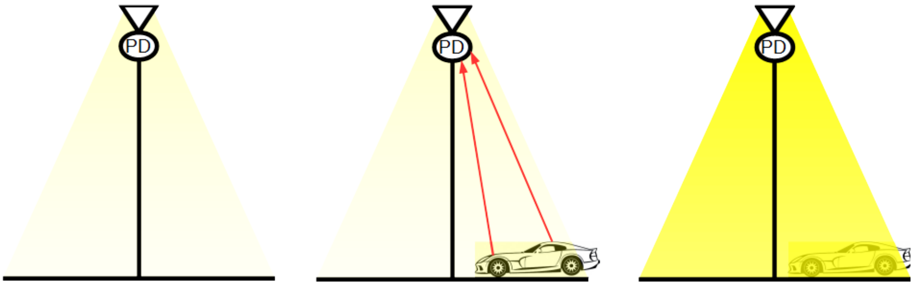

Figure 1.1: When no object is in the area, the luminaire will barely generate any light. If an object drives into the area, the reflections will be picked up by the photodiode, which will then turn the light on.

sumes any energy while nobody is around but is still able to detect people, cars or other objects passing by. It might even be possible to decrease the light output to an amount which is invisible to the human eye, resulting in an unnoticeable, activity detecting, energy-saving device.

1.1 Problem statement

Is it possible to create a system which can detect the activity of humans or objects by measuring reflections of visible light while being invisible to the human eye?

This problem can be divided into three sub-questions:

- How strong is a reflection obtained from a flash in a realistic scenario and how much does this reflection change if an object enters the area?
- What are the challenges in obtaining reflections when using a low-intensity light and how can they be tackled?
- What additional signals are received by the system (noise) and what algorithm can be used to convert the received signal in a reliable logical signal: Detection or no detection?

1.2 Contributions

This thesis proposes **Dark Sensing**, a system that uses reflections of an LED controlled with a low duty cycle (4%), and therefore nearly invisible to the human eye, to detect changes in the surrounding area.

- A model, estimating the change in signal (reflected light) when a object moves under, leaves or passes by the LED in different environments.

- A method to convert a captured reflection of the LED into a usable measure of the environment.
- An algorithm which analyses features of consecutive flashes and is capable of detecting objects moving under, leaving or passing through the illuminated area.
- A prototype capable of detecting between 73% and 90% of all humans passing by in a realistic environment dependent on the allowed false positive ratio (0 - 5%).

1.3 Organisation

This thesis describes the development path of the new technique "Dark Sensing" from idea to a working prototype. Chapter 2 will present the required background knowledge to understand several choices made in this thesis and present the related work. In chapter 3 a model will be presented, which calculates the theoretical response of bypassing objects. Chapter 4 describes the created experimentation platform. Chapter 5 will focus on finding the ideal settings for generating an analysable flash and will explain what the best method is for extracting data from this flash. Chapter 6 explores the possibilities for analysing sets of consecutive flashes and proposes an algorithm to detect significant changes in the signal. Chapter 7 tests the prototype created and evaluates the performance of system. The thesis concludes with an evaluation of the new "Dark Sensing" technology and suggests several possible directions for future work.

Chapter 2

Background and related work

2.1 Background

This section presents the required field knowledge to understand this thesis. It therefore starts with an explanation on how a light source behaves when it turns on and off rapidly and why this is preferable over other light saving strategies. It then follows up with an explanation of how light beams travel and reflect off of surfaces.

2.1.1 Dimming of an LED

In this thesis, an LED will be used to illuminate the environment which will cause reflections in the room. It's therefore important to understand how the light responds to different methods of adjusting the light output, as this directly influences power of the reflections.

In general, there are two methods of dimming (reducing the light output of) an LED: Analogue and digital. A light which is dimmed in an analogue manner has its total light output reduced by reducing the current flowing into the LED. This leads to a light which has a constant light output directly proportional to the current flowing into the LED. If we for example want a light to produce 25% of its normal light output, we simply supply it with a quarter of the current. A graphical representation of analogue dimming is shown in Figure 2.1(a) and is marked as ”average power”.

Digital dimming works in another way. Instead of controlling the amount of current flowing into the LED, we control the amount of time current is allowed to flow into the LED. This can be achieved by turning the LED on and off rapidly. If we for example want to reduce the light output of an LED to 25% with the help of digital dimming, then we would turn the light on at full strength for 25% of the time, while turning it off for 75%, with the help of a Pulse Width Modulated (PWM) signal. A graphical representation of digital dimming is shown in Figure 2.1(a).

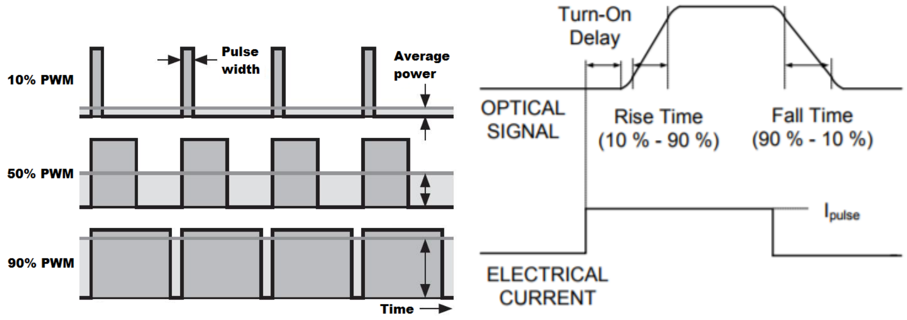

(a) (b)

Figure 2.1: Figure (a) shows the difference between analogue and digital dimming, Figure (b) shows a realistic response of the light when a short electric pulse is applied[7].

The resulting light produced by both types of dimming are indistinguishable for humans if the switching frequency of digital dimming is high enough. Both methods have the same apparent brightness and use the same amount of power. For photodiodes however, there is a clear difference. The analogue signal will show up as a constant, but weak signal. The digital signal shows up as a square wave with high peaks (when the light is on) and valleys (when the light is off). This becomes especially apparent if we want the system to work at only 1% of it's original illumination level. The signal dimmed in an analogue manner will be nearly invisible as it is turned on constantly at 1% of it's original power. This in contrast to the digital signal, which only shows up for 1% of the time, but at maximum power, resulting in a shorter but much brighter peak. Because the 1% time constrain is no problem for an electronic system, it was chosen to explore Dark Sensing with this dimming method.

There is however a limit to how much the energy consumption can be reduced with digital dimming, if we want to be able to observe the signal with a photodiode. When an LED is turned on, it does not produce light at maximum intensity instantly[7]. It first has a short "turn-on delay" where the light does not output any light, followed by a "rise time" where the light "slowly" powers up until it has reached it's desired intensity level. A graphical representation of this process can be seen in figure 2.1(b). This limit on digital dimming forces a hard minimum to the amount of digital dimming the system can work with and therefore limits the amount of energy it can save.

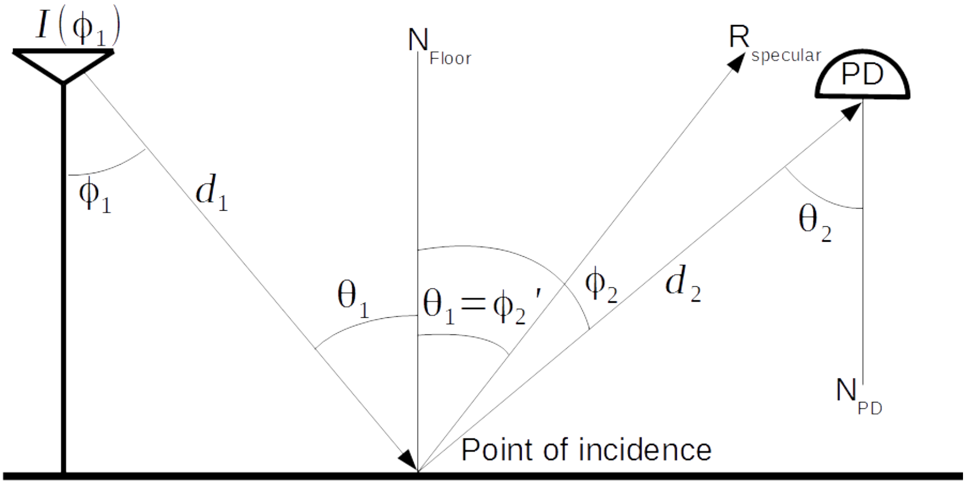

Figure 2.2: Overview of angles, vectors and distances used in the model. It represents a street light illuminating the street (I). This light is then observed by a photodiode (PD), aimed at the ground. Note that ϕ always represents an exit angle and θ always represents an incidence angle.

2.1.2 The Phong model

When a light shines on a surface, some parts of the surface appear brighter than other parts. This is caused by three major factors:

- The light used to illuminate the wall and it's position relative to the wall.
- The surface of the wall itself.
- The position of the observer relative to the wall.

If all of these factors are known, then the complete pathing of the light can be approximated with the help of the Phong model. This section presents a simplified version of the Phong model which is used in chapter 3. All used angles can be seen in Figure 2.2. The full model can be found in [17].

Modelling an LED

A light can be modelled if several parameters of the light are known, with the help of equation 2.1. This formula describes how much light is leaving the light source at angle ϕ relative to the normal of the LED.

$$I(\phi) = \Phi_{lum} \frac{\alpha + 1}{2\pi} cos^{\alpha}(\phi_1) \tag{2.1}$$

The equation consists of three parts. Φ_{lum} represents the total amount of light emitted in lumen by the LED. $cos^{\alpha}(\phi_1)$ represents the radiation pattern of the LED. α represents the order of Lambertian emission which describes the illumination pattern of the LED. If α is low (e.g. 1), then this equation

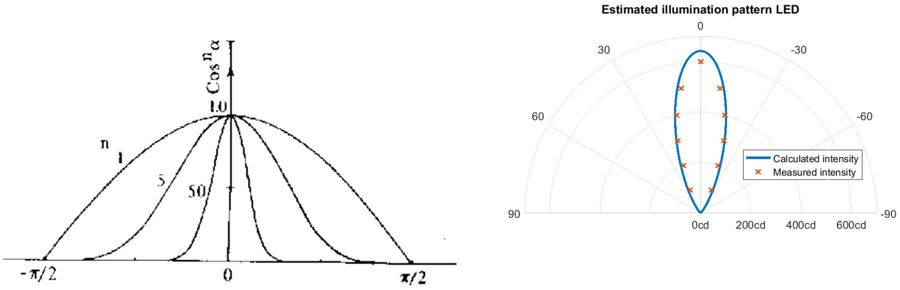

(a)

(b)

Figure 2.3: (a) shows an overview of how adjusting α changes the light cone of a simulated light source. (b) shows a modelled light cone, modelled with the shown measured light cone.

represents a luminaire with a very wide spread of light, for example a street light. If α is high (e.g. 200+), then the light source is much more focused like a laser. An overview of α values versus their angle is shown in Figure 2.3. $\frac{\alpha+1}{2\pi}$ is a normalisation factor that ensures that integrating equation 2.1 results in the total amount of light produced (Φ_{lum}), as reshaping the cone of light with α would otherwise lead to a change in produced light. An example of a modelled light with $\alpha = 14.3$ and $\Phi_{lum} = 260lm$ can be seen in Figure 2.3(b).

We can now take any light ray from the luminaire and calculate how much light hits a specific surface with the help of equation 2.2. This calculation also consists of three parts. The first part is, $I(\phi_1)$, the strength of the light ray calculated with equation 2.1. The second part, d, represents the distance the light needs to travel before it hits the surface. The final variable, θ_1, represents the incidence angle of the light ray on the surface.

$$E_{hor} = \frac{I(\phi_1)}{d^2} cos(\theta_1) \tag{2.2}$$

Modelling a reflection

Light impinging on a surface can reflect in three different ways: Diffuse, spread and specular. Almost all surfaces combine several of these reflection types. A visualisation of these reflections can be seen in Figure 2.4. The **specular reflection** is a so called perfect reflection. It reflects each incident ray outward, with the reflected ray having the same exit angle to the normal vector N as the incident ray. A material with this kind of property is a mirror. The **diffuse reflection** is the opposite. Instead of reflecting light in one direction, the light ray is scattered in all directions following

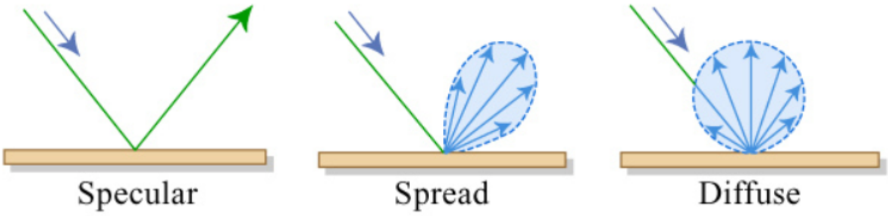

Figure 2.4: The possible ways for light to reflect when it hits a surface [1].

a Lambertian emission pattern. This leads to a point, which appears to have the same brightness, no matter the observation angle. A common material with this property is plain white paper. The final kind of reflection is the called the **spread reflection**. It's a scattered reflection, aimed in the direction of the ideal reflection. A material which has mainly this kind of reflection is matte aluminium.

All of these reflections can be modelled with the help of equation 2.3, where ϕ_2 represents the observation angle. The first part of the equation calculates how much of the impinging light is reflected off the surface and not converted into heat. This is determined by A, which represent the albedo of the observed surface.

The second part describes the actual reflection of the surface. $\frac{\alpha+1}{2\pi}\cos^{\alpha}(\theta_1' - \phi_2)$ describes the spread reflection and is modelled as a light source pointing in the direction of the ideal reflection θ_1' (see equation 2.1). The higher α is chosen, the more focused the reflection. If α is chosen to be infinite, the surface is modelled as a mirror instead.

$\frac{1}{\pi}\cos(\phi_2)$ describes the diffuse part of the equation and is also modelled with 2.1 where $\alpha = 1$. This results in a diffuse reflection. The final term of the equation is r_d. This value represents the ratio between the diffuse and spread reflection.

$$R(\theta_2) = E_{hor}\rho(\lambda)\left[r_d\frac{1}{\pi}\cos(\phi_2) + (1-r_d)\frac{\alpha+1}{2\pi}\cos^{\alpha}(\theta_1' - \phi_2)\right] \tag{2.3}$$

Modelling a photodiode

The final part missing in the model is the observer. The observer, or receiver in our case, is a photodiode which can be modelled with the help of Equation 2.4. This equation is very similar to equation 2.2, but has one major difference: The $rec(x)$ function. This function checks if the light incoming at angle θ_2 lies in the field of view of the photodiode. If it is, then $rec\left(\frac{\theta_2}{FOV}\right)$ returns 1, otherwise it's 0 and the ray of light wont be counted.

$$PD = \frac{I\cos(\theta_2)}{d^2} rec\left(\frac{\theta_2}{FOV}\right) \qquad rec(x) = \begin{cases} 1, |x| \leq 1 \\ 0, |x| > 1 \end{cases} \tag{2.4}$$

Creating a 3D model

All equations shown in the previous sections can be combined into one big equation, calculating how much a point on the wall is illuminated, reflected and perceived by the observer. This equation is 2.5. It has however a lot of variables, which will make it hard to create a proper simulation.

$$PD_{tot} = I(\phi, \alpha_{light}, \Phi_{lum})R(\theta_1, \phi_2, \lambda, r_d, \alpha_{floor})PD(\theta_2, d_2) \tag{2.5}$$

This can be solved by making the problem concrete and simulate it in a 3D space with an xyz coordinate system. If we assume the floor is a plane spanning x and y (thus z = 0) and fix the positions and normals of the LED and photodiode, we can express all angles and distances as formulas of x,y and z. If we then want to calculate the total amount of energy perceived by the photodiode, all we need to do is integrate over all the points of the floor (the xy plane).

$$PD_{tot} = \int_x \int_y I(x, y, z, \alpha_{light}, \Phi_{lum})R(x, y, z, \lambda, r_d, \alpha_{floor})PD(x, y, z) \tag{2.6}$$

This model was used to create the model used in chapter 3. That chapter will also explain what changes were made to obtain the presented model.

2.2 Related Work

This section presents the related work of this thesis. It starts with giving a short overview of several methods used for passive localisation. It shows the projects which use visible light in their localisation schemes. This section finalises by highlighting a paper which attempts to reduce the visible light used in a similar way to this thesis.

2.2.1 Passive localisation

Passive localisation is a hot topic in research and has been tackled by many different research groups in several different ways. The most common method found in literature to detect and track humans is by using Passive Infra-Red (PIR) sensors. These sensors detect the infra-red (heat) radiating from objects and draw conclusions from the observed signals. The passive infrared sensor has been around since 1982 [5] and has been used to detect humans since 1994 [10].

These days, the research in PIR sensors for detecting and tracking humans focuses in two directions. The first direction is to get more information out of PIR sensors by examining the raw data. M. Waelchli *et al.* for example created a method for estimating the location of a person within the view of the sensor [11]. The second direction is to track humans with the help of several linked sensors. An example of this, by P. Zappi *et al.* is [18]. They linked a server to multiple binary human activity sensors, in order to locate and track humans in an indoor building.

Another method for passive localisation, which popped into existence more recently, is developed by M. Youssef *et al.*[16]. They created a detect and track application with the help of WIFI access-points (APs), WIFI monitoring-points (MPs) and an application server (AS). The MPs measure the signal strength of the APs, and transmit this data to the AS. The server runs a moving variance algorithm on all of the received signals to detect significant changes in the signal.

Another approach to passive localisation is to use the tiles upon we walk as sensors. This was done by M. Valtonen *et al.* [14]. The system measures the capacity between several floor tiles and a receiving electrode. With the help of the measurements, they estimate the position of the person standing on top of the tiles.

2.2.2 Passive Visible Light Localisation

In recent years, a new method for locating and tracking humans has been explored: Passive Visible Light Localisation (PVLL). This method is focussed on using visible light and photo sensors to detect and track humans and objects. Several of these project will be explained briefly, followed by a

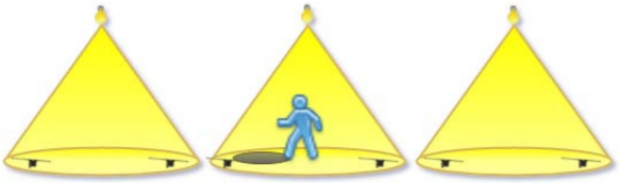

Figure 2.5: Overview of the LocalLight system of E.D. Lascio *et al.*[4]. Lights on the ceiling and light sensing RFID tags on the floor.

short comparison between these projects and Dark Sensing.

Local Light

Local light, developed by Lascio *et al.*[4], is a system which implements passive localization with the help of visible light. The system consists of 3 parts. A light, light sensing RFID tags and a server. The light illuminates the environment. The RFID tags are mounted in the floor, detecting the light produced by the luminaire. The tags transmit their data to a server which processes the data. An overview of the system can be seen in Figure 2.5.

The system works by detecting changes in the light intensity. If the photo diode suddenly senses a huge drop in light, because a shadow is casted on the photo diode by an object or person, the system triggers a detection. The server knows the exact location of all luminaries and photo diodes and is therefore capable to of determining where the object or person is at this moment in time.

Activity sensing using ceiling photo diodes

Three different projects have been found which have develop a passive localisation scheme using several light/photo diode pairs mounted together on the ceiling. Both take a slightly different approach.

The first project, by J. Zhang [19], created a method capable of localising objects on a line between two light/photo diode pairs. By moving an object with three reflective surfaces underneath a light, he managed to localise them at several points on the line by using the specular component of the reflections bouncing of the object. His test set-up can be seen in figure 2.6.

The second project, by M. Ibrahim *et al.* 2.7, makes use of modulated lights. Each luminaire transmits light in a different pattern. The photo diode, which is placed next to the light, detects what patterns of light it perceives. If the photo diode does not sense one of the lights it normally does, it triggers a detection as the light was intercepted by a bypassing object. An overview of the set-up can be seen in Figure 2.7/

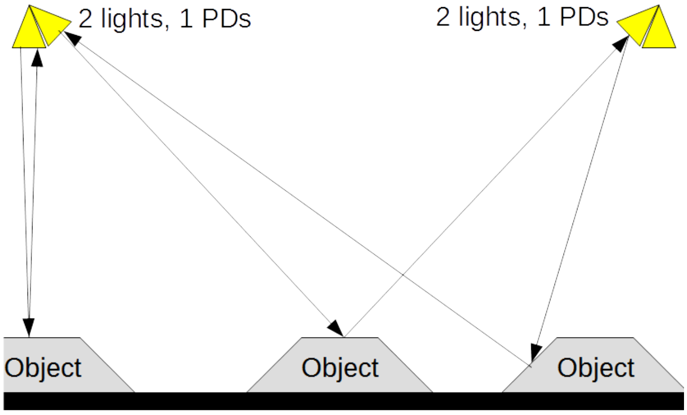

Figure 2.6: Overview of the system used by J. Zhang [19]

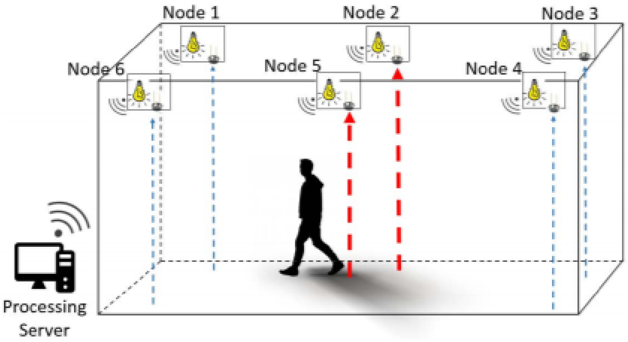

Figure 2.7: Overview of the system set-up used by M. Ibrahim[15]. In this specific situation node 2 and 5 detect no light from node 1, because a person is blocking the light.

Comparison with Dark Sensing

The Dark Sensing project differs from the existing projects in several ways. It's the only project tempting to create a sensing device, only requiring one sensor node instead of multiple and is therefore easier to install and expand. It's also the only project which attempts to save energy. It's also the only project which potentially can be implemented outdoor, mounted on a light post for example, as the other PVLL projects where require either a server in reach of the sensors, or other specific environmental features. Dark Sensing has the potential to be a stand alone product.

The downside of Dark Sensing is that it only focuses on detecting activity. It's therefore unable to track users. All of the other projects are way better in that specific area.

2.2.3 Other related projects

One project that is not related to passive localisation, but inspired us to use short pusles of light is *"The dark light rises"* by Z. Tian *et al.* [20] [21]. This group explores the idea of Visible Light Communication (VLC) with dark light, a VLC primitive that allows light-based communication to be sustained even when LEDs emit extremely-low luminance. The communication works by generating high power, but short light pulses (500ns). These pulses are then used in a pulse position modulation scheme to achieve communication (1.8Kbps at 1.3m) with light while being nearly invisible to the end user. The goals of Dark sensing and Dark VLC are similar: Save light and therefore energy. Both projects however apply this method in different applications.

Chapter 3

Model

A model has been made with the goal of answering two questions:

- How strong are the reflections of flashes in a realistic environment?
- How and how much, will these reflections change if an object enters the illuminated area

This section uses the model explained in section 2.1.2. It starts by distinguishing the changes made to the original model [17] and shows that the model gives a reasonable estimation of reality. It then describes two modelled scenarios and presents the results. The chapter ends with answering the posed questions.

3.1 Model description

The model made is an interpretation of the Phong reflection model (see section 2.1.2). It calculates how much of the light leaving a luminaire, bounces back via the environment to a photodiode placed next to the light source. This section will first discuss the adjustments made to the Phong model, followed by an explanation of the simulation process.

3.1.1 Model Adjustments

The model presented in section 2.1.2 is not the complete Phong model. Several parts where simplified or removed as they should barely influence the results of the simulation.

The first adjustment is the removal of "time". The methods in the literature took the travelling time of light into account in order to calculate the possible inter-symbol interference. This is not required for this simulation as we are only interested in the steady state situation when the light is fully turned on and the light received by the photodiode is maximized for the current situation.

The second adjustment is the removal of "colour". The original method differentiated between different wavelengths of visible light, while producing, reflecting and receiving light. It was therefore maintaining colour information. This is however not necessary for this model, as we do not care about the colour of the reflecting objects, but only about the total amount of energy reflected by the object. For this reason, the surface reflection coefficient ($p(\lambda)$) was replaced with the albedo of the object instead (A).

$$\Gamma = \int_{380nm}^{780nm} \Phi_e p(\lambda) d\lambda \rightarrow \Gamma = \Phi_{lum} A \tag{3.1}$$

Albedo is a property of an object representing the ratio of energy which is reflected when sun is shining on it. Even though albedo is based on the full spectrum of sunlight instead of only the wavelengths of visible light, it gives a reasonable approximation of the reflection coefficient in this scenario. This is shown in section 3.2.

The final adjustment is the amount of reflections we calculate. In reality a light ray can be reflected an infinite amount of times of off several different surfaces before returning back to the sensor. In the model however we only calculated one bounce (from the light to an object and back). The reason for this is that the first reflection provides approximately 80% of the signal where all other reflections only make up 20% of the total power[12]. If we where to add multiple bounces, the accuracy of the model would only increase by a maximum 20%. Adding the extra bounces makes the model many more times complicated, depending on the environment we are simulating. A simple hallway model would be 8 times as complex to model and require at least 4 times as much computation power, while only providing "only" 16% more accuracy.

3.1.2 Calculation process

Calculating the amount of light reflecting back to the object is a three step process. The first step is to calculate the shadow casted by the object on the floor and walls. This is required as the surface where the shadow is casted can't reflect light back directly to the photodiode. It's important to note that the light casting the shadow is reflected of the object instead and with that, changes the reflection pattern of the room.

The second step is to calculate how much light reflected from all floors and walls (where no shadow is casted) is received by the photodiode. The final step is to calculate how much light is reflected from each side of the object. Figure 3.1 shows an overview of an environment with rays leaving the light, casting shadow and the resulting reflections.

3.2 Verification

The calculation method and changes in the model where verified using a scale model featuring a LED[9], a paper box and a light meter[13]. The first

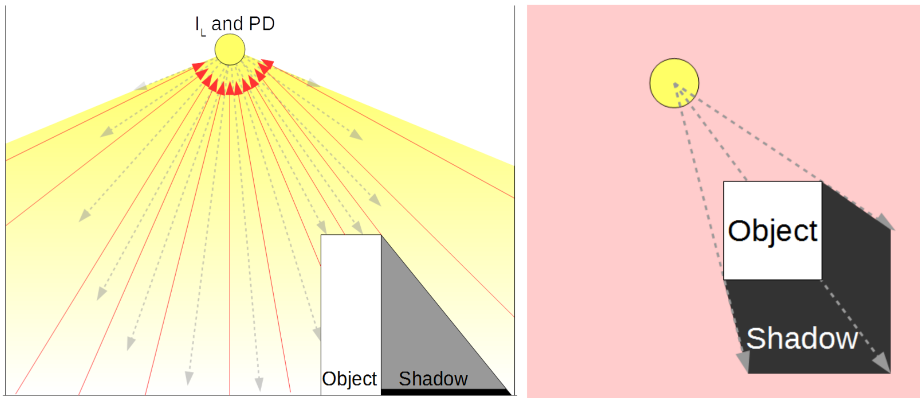

(a) Sideview (b) Topview

Figure 3.1: Overview of the calculation process. Grey lines represent light rays casted by the light. Black represents the shadow casted by the object on the floor or walls. Red lines or areas show reflections bouncing from the ground, walls or object back to the photodiode.

step of verifying the model is to check if the LED is modelled properly by equation 2.1. This was done by hanging the LED at 100cm above the floor and measuring the horizontal illuminance (E_{hor}) at the floor to see if the measured irradiation pattern of the LED matches the theoretical pattern produced by equation 2.2. Measurements and simulations in Appendix A show that the LED in the test set-up was producing more light than in the specification. These numbers where therefore adjusted for the next step of verification.

The second step is the verification of the interpretation of the Phong model. This was done with the test set-up shown in Figure 3.2. By moving a paper box across a paper covered floor in steps of 5cm and measuring the reflections in each step, we obtain the red line in figure 3.3(a). When we compare this line with the blue line generated by the model using $A = 0.75$ (albedo of paper according to [6]), then the lines closely match.

The test was repeated using the original floor of the room. The albedo of the floor was calculated to be 0.37, based on a measurement of the floor without the paper box. The result of the second test can be seen in Figure 3.3(b). The resulting curves also seem similar. As the model has shown to reflect reality quite closely, it seems fine to assume that the model works and can be trusted some extent. It won't give exact results, but it will al least provide a proper approximation of the perceived light.

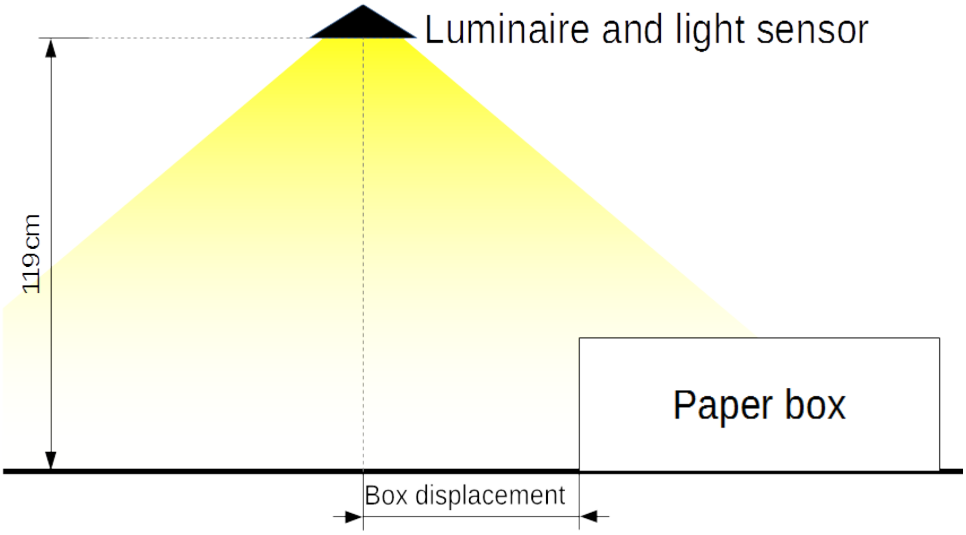

Figure 3.2: Visualisation of the model verification set-up.

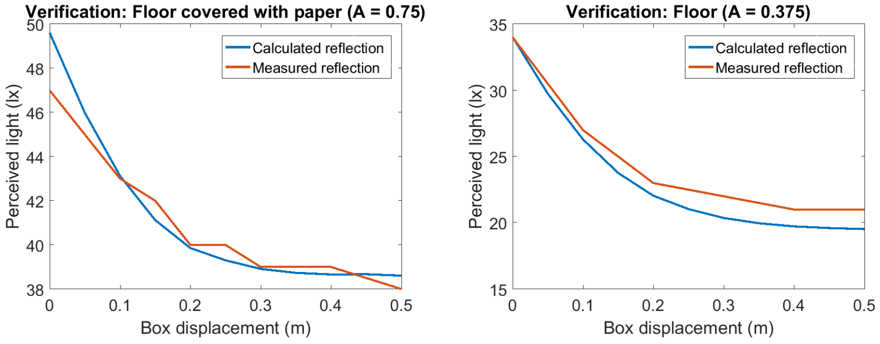

(a)

(b)

Figure 3.3: Both figures show that the model provides a reasonable approximation of reality. Note that the albedo of paper was taken from [6] and the albedo of the floor was estimated with measurements.

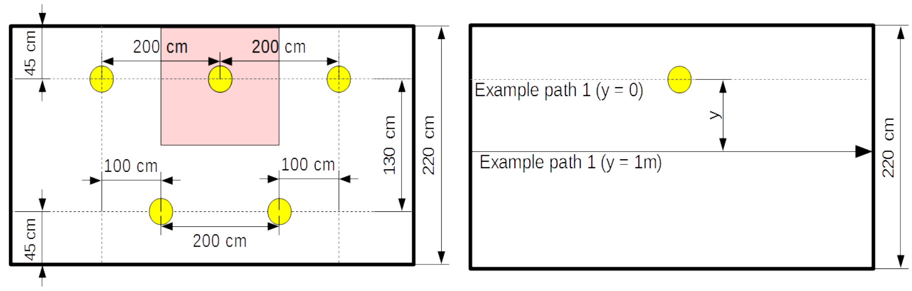

(a) Staggerd hallway LED pattern

(b) Traveling path of the object

Figure 3.4: Figure (a) shows the position of the luminaires to obtain a realistic illumination pattern. The red square represents the area one light/photodiode pair should cover. Figure (b) shows an example travelling path of an object.

3.3 Modelling of the hallway

The hallway modelled is based on a real hallway located at the TU Delft. The hallway is 2.2m wide and 2.8m high. The floors albedo is set at 0.37, as this was calculated during the verification of the model. The albedo of the walls was set to 0.95 which represents the albedo of white plaster[6]. The reflection of these surfaces is assumed to be fully diffuse ($r_d = 1$).

Industry standards state that corridors in education buildings should be illuminated with at least $E_{mean} > 100lx$ and a light uniformity of $U_o > 0.4$[22]. E_{mean} represents the mean illumination level of the floor and U_o the proportional difference between E_{mean} and $E_{minimum}$. These lighting requirements can be achieved using the same luminaire used during the verification process if hung in the staggered formation shown in figure 3.4(a). Calculations showing that the industry standards are met can be found in Appendix A.

$$E_{mean} = \frac{1}{y \cdot x} \int_y \int_x E_{hor}(x, y) dy dx \qquad U_o = \frac{E_{mean}}{E_{minimum}} \tag{3.2}$$

The object passing by the light (representing a human) will be modelled as a cuboid 0.2m wide and 0.5m long with varying heights. Several albedos have been assigned to the cuboid to represent the different kind of clothing humans wear. The object will be moved in a straight line trough the hallway with the light at a set vertical distance y. Some example paths can be seen in Figure 3.4(b).

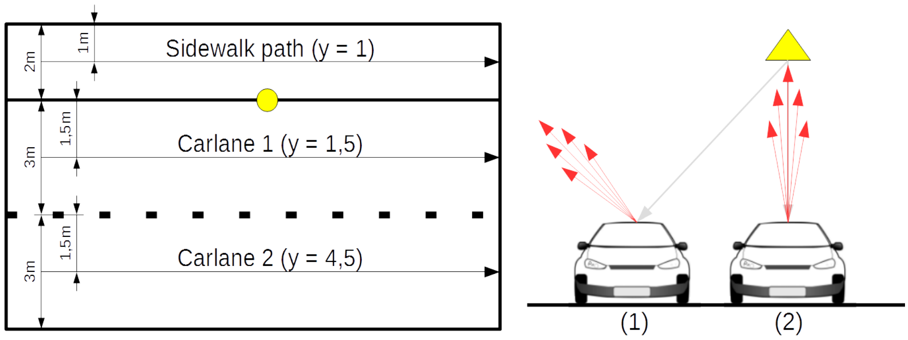

(a) Topview of the street model

(b) Spread reflection on cars

Figure 3.5: Figure (a) shows an overview of the model. Figure (b) shows that a spread (or specular) reflection will only reach the light in situation (2). This situation does not occur in the modelled scenario.

3.4 Modelling of the street

The street model is based on a real street near the TU delft. It has two lanes for cars (each 3m wide) and sidewalk (2m wide). The albedo of the street will be modeled with $A = 0.11$ which represents old asphalt[6]. The reflections of the street are assumed to be fully diffuse ($r_d = 1$).

Industry standards state that a street with side walk should be illuminated with at least $E_{mean} > 3lx$ and a light uniformity of $U_o > 0.2$ [3].These lighting requirements can be achieved using 700lx luminaires with a half power angle of 60° ($\alpha = 1$) placed every 15 meter in between the road and side walk. This set-up is visualized in figure 3.5(a). Calculations showing that the industry standards are met can be found in Appendix A.

In this model two different objects will be modelled representing humans (walking on the side walk) and cars (driving in the two driving lanes). The humans will be modelled in the same way as in the hallway scenario. The car will be modelled as a cuboid with the dimensions of an Opel Corsa (4m x 1,7m x 1,5m), a commonly seen small car. The objects where modelled with diffuse reflection, because no reliable sources describing the reflection parameters (r_d and α) of cars could be found.

Lacking the specular and spread reflections for this specific model should not influence the results significantly, as no part of the car will be moved directly underneath the light and therefore no significant amount of light of the spread reflection should ever reach the light sensor. This is visualized in figure 3.5(b).

3.5 Results

Several simulated measurements have been plotted in Figure 3.6. All plots can be observed with the tools provided by appendix A. The plots on the left side of Figure 3.6 show the best (most deviation from steady state) and worst case (least deviation from steady state) scenarios for the simulated situations.

In general we can state that the extremer the albedo, the better the bypassing object can be observed. A high albedo leads to a huge peak in the signal. A low albedo leads to a huge drop in signal as most of the light otherwise bouncing back to the source, is now absorbed by the object itself. Another thing which can be observed is that the smaller the y distance, the better the signal can be observed.

If we look specifically at the worst case scenario for the hallway (Figure 3.6(c)), we can see that the signal changes 0.1lx when a small person with low albedo is simulated. Even though a signal of 0.1lx is a low absolute value, the change in signal is 3% from the steady state, which should be detectable with a correctly configured photodiode. The same goes for cars driving in the street (Figure **??**. Almost all of the bypassing cars should be detectable, at least in lane 1, as the proportional change is at least 6%. Detecting humans walking on the street seems however out of reach for this project, as the relative change in signal is less than 0.5%.

Figures 3.6(b), 3.6(d), 3.6(f) and 3.6(h), show the frequency spectrum of the received signals. They where obtained by calculating a Fast Fourier Transfrom (FFT) over the signal with an F_s (sample rate) by assuming a constant movement speed, $5km/h$ for humans and $30km/h$ for cars, over the observed area. These plots show that the frequencies, carrying the signals, lie between 0.1Hz and 2Hz for all simulated cases.

3.6 Conclusions

In this chapter, a version of the Phong model was implemented, verified and used to estimate the light response if a person or car would move past a light/photodiode pair. These responses gave several insights:

- The extremer the albedo compared to the environment, the better the bypassing object can be detected.
- Detecting bypassing humans in the hallway is possible, because the relative change in signal when a human passes by is at worst 3%.
- Detecting cars driving in a lane next to the light is probably possible, as the change in signal is at least 6%. Detecting cars in the second lane is harder, but might be possible unless the car has a similar albedo as the reflecting background.
- The expected frequency of the signal lies between 0.1Hz and 2Hz for both the street and the hallway scenario, no matter what properties

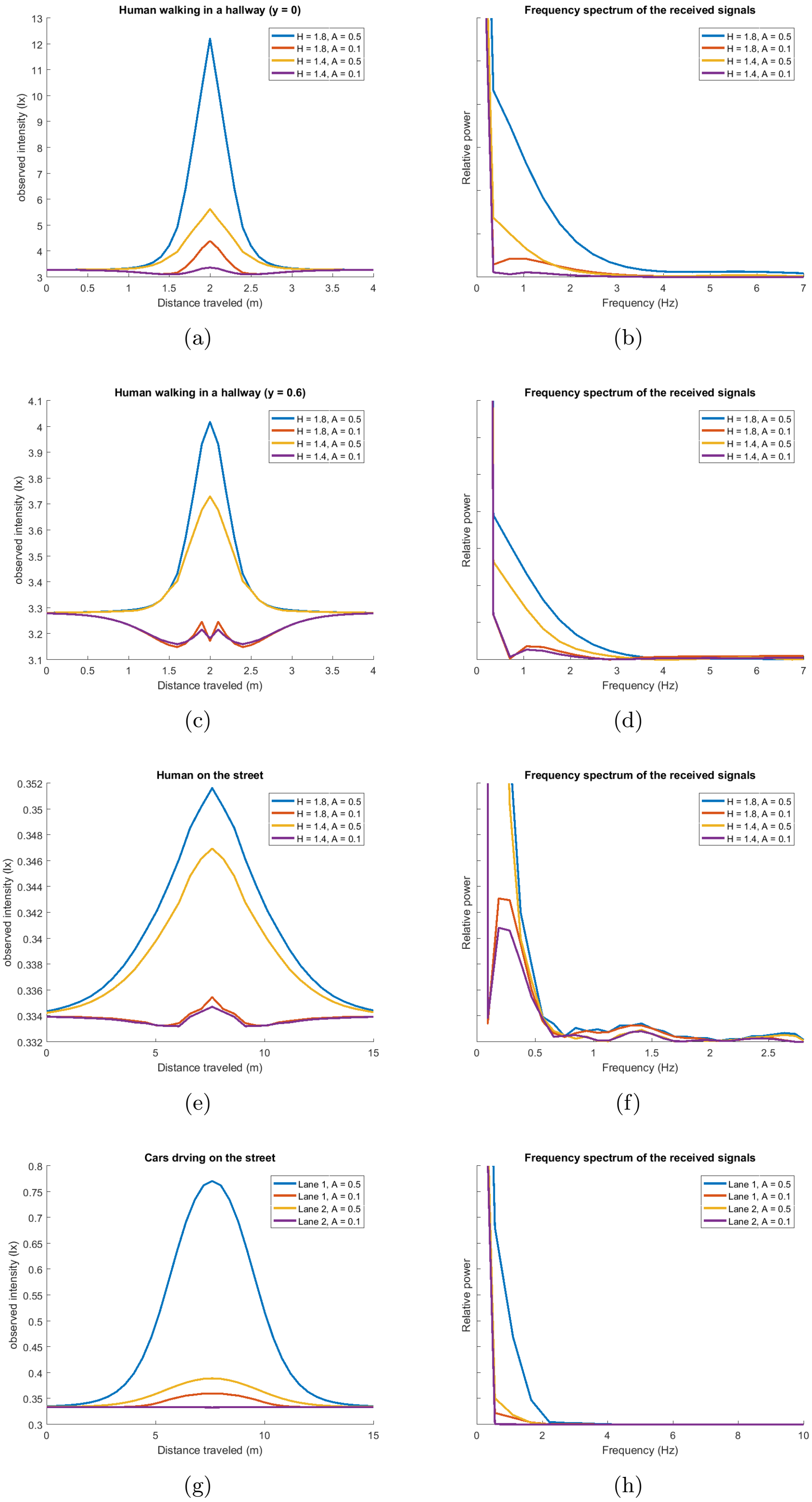

(a)

(b)

(c)

(d)

(e)

(f)

(g)

(h)

Figure 3.6: Several selected simulated responses. The left figures show the biggest and smallest responses. The right figures show the frequency spectrum of those signals.

the object has.

The insights obtained with this model will be used in several places later on in the thesis.

Chapter 4

Platform

A device has been made to generate, receive and analyse flashes. The complete system architecture is shown in figure 4.1. Each component and their interfaces will be discussed briefly, followed by a section describing the final build of the platform.

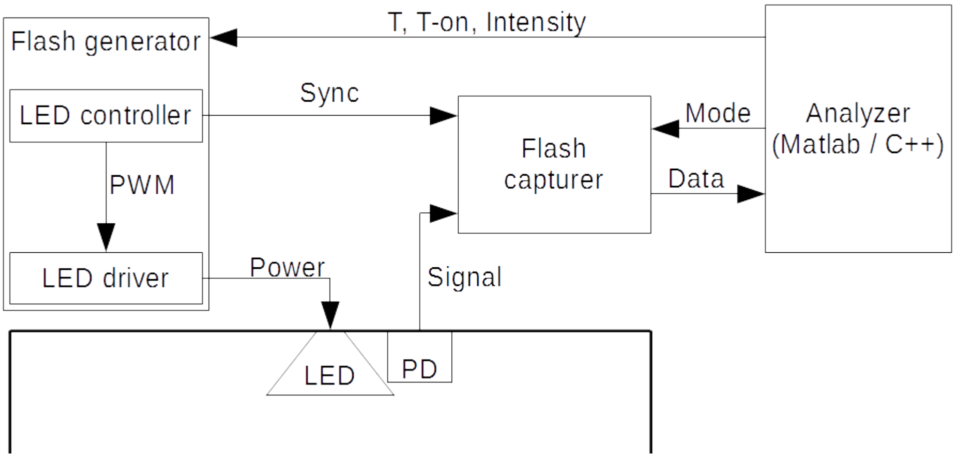

Figure 4.1: System architecture of the created platform.

4.1 system components

4.1.1 Flash generator

The flash generator is a device able to control a LED with high precision. It's able to set the period T, and the t-on time T_{on}. T controls the frequency of the flashes and T_{on} the length. Both parameters can be set with a resolution of $10\mu s$ resulting in a precisely controlled PWM signal with the help of equation 4.1. This signal is sent to a LED driver through one of three LED

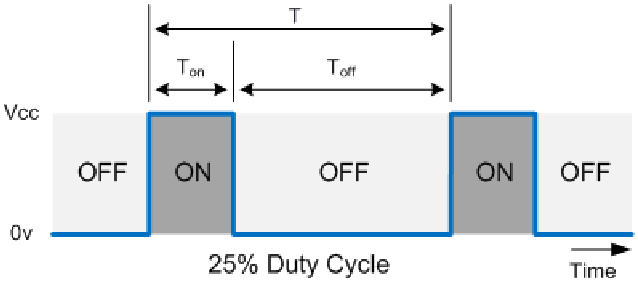

Figure 4.2: Visualization of how T and T_{on} determine the duty cycle and frequency of the flash generator.

drivers, which will make the actual light turn on and off at different light levels.

$$T = \frac{1}{f} \qquad DutyCycle = \frac{T_{on}}{T} * 100\% \tag{4.1}$$

Besides generating the PWM signal for the light, the flash generator has another function. It sends a sync signal to the flash receiver just before generating a flash. This allows the flash receiver to be ready when the flash starts, so it does not waste time sampling if no flash is generated.

4.1.2 Reflection receiver

The job of the receiver is to sample values while the light is being turned on and off, to then analyse the full reflected flash and extract a feature which properly represents the environment. The receiver should therefore capture flashes as precise and consistent as possible. For this reason, the receiver receives a sync signal from the flash generator and is therefore able to start sampling at almost the same moment every time, relative to the start of the flash.

The receiver should continue sampling for a set period of time. Once done, the device should do one of the following things with the received samples, depending on the mode of the analyser:

1. Send back the full flash, uncompressed, for the analysis of separate flashes.
2. Send back all compressed flashes, by extracting several features.

4.1.3 Analyser

The analyser will receive samples from the reflection receiver and is ran on a PC in the form of either a C/C++ program (real-time) or as a MATLAB script (post-time). The analyser can set the receiver to work in *raw* or *compressed* mode. If the receiver sends raw flashes to the analyser it can be used to analyse these flashes in detail. This mode is used in chapter 5 to analyse single flashes in order to find the ideal settings for the flash generator and reflection receiver. If the receiver sends compressed flashes, the analyser is able to analyse consecutive flashes. This mode will be used in chapter 6 to find an algorithm to determine if an object is moving in the area under the light.

The Analyser should also be able to control the flash generator if the system is running in real-time mode. It is therefore able to send a packet with T, T_{on} and I_{LED} to the device. This allows for real time control of the flash generator.

4.2 Implementation

The system was build by combining several off shelf components. An overview of the actual platform can be seen in figure 4.3. It shows the different components mounted on a box. This section will explain briefly how each system component is implemented and why each part was chosen.

The flash generator is implemented on an Arduino UNO[2]. This platform was chosen, as it's simple to use, does not require an operating system (OS) and has therefore no unexpected jitter. The LED used in the set-up is the same LED as modelled in chapter3. The power used by the LED is regulated with a single resistor. The resistors where chosen after some experimentation with the flash generation and reception. The values and resulting LED current can be seen in equation 4.2.

$$I_{LED} = \frac{V_{DD} - U_{LED}}{R} \qquad I_{LED} = \frac{7 - 3.6}{[1, 3, 5]} = [3.4A, 1.1A, 0.68A] \tag{4.2}$$

The reflection receiver is implemented on the shine platform [8]. This platform was chosen because it's a simple (no OS required) hands-on platform featuring multiple photodiodes by default. The original software of shine sampled each photodiode at 1Khz. This is way too low to see the $10\mu s$ flash resolution. For this reason the software of shine was rewritten to sample in bursts of 50 samples at 210Khz (for a total of$\pm 240\mu s$) when the sync signal is received.

A downside of the shine platform is that it's unable to communicate directly with the analyser as it does not has a FTDI interface. This problem was solved by using a processor-less Arduino UNO as bridge between the analyser and shine platform.

The receiver makes use of three photodiodes of which it will use one at a time. The original sensors on shine where replaced with ones more sensitive to visible light. Each sensor is configured in a different way. Some feature an increased amplification of the measured signal. Others have a longer wire

PD#	Wire length	Gain	EMC Shield
1	Long	1000	Slecteable
2	Short	5600	Yes
3	Short	10000	Yes

Table 4.1: Overview of photodiode configurations.

with (intentional) bad shielding which can simulate how the system preforms in a environment with lots of electromagnetic radiation. An overview of the PD configurations can be seen in table 4.1.

Another important decision concerns the amplification circuit of the photodiode. The original circuit used by shine uses an analogue low-pass filter to remove ripple introduced by the amplifier (See Figure 4.4). The filter has several side effects. It reduces the signal strength and decreases the time the signal is visible to the system. It was therefore chosen to remove al analogue filters from shine and deal with the ripple with the help of software if required. The ripple effect might even be useful as the it's probably dependent on the received signal strength and therefore a measure of the environment.

4.3 Summary

The system has been built and tested. Even though the created device has a poor build quality, it has great potential for experimentation with the proposed method of activity detection. The main advantages are:

- Each building block has one clear purpose and can therefore be tackled separately from other components. It's therefore impossible that a timing error in the flash generator software affects the sampling of the receiver or vice versa.
- The build quality is poor. If the project works on this device, it will definitely work on a dedicated platform.

The next steps for the project is finding a method for extracting useful information from flashes as shown in figure 4.4(a).

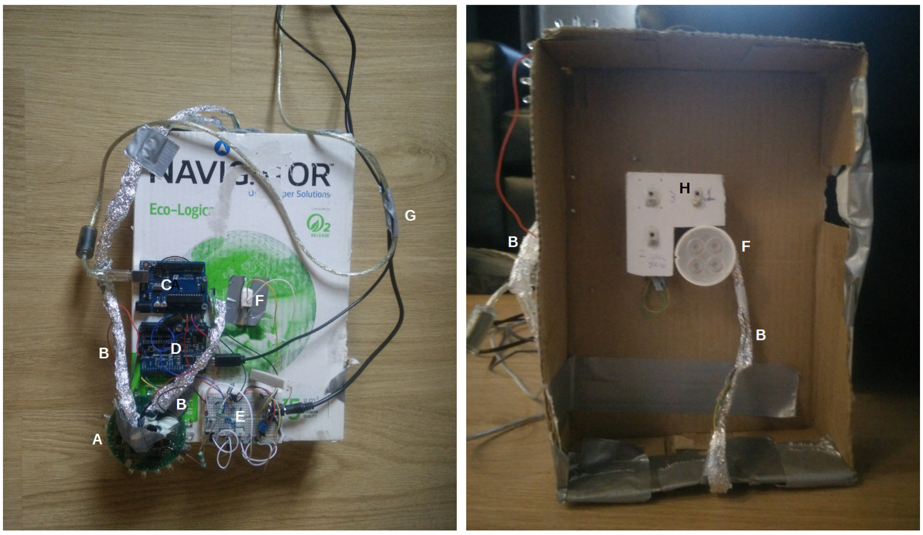

(a) Top view

(b) Bottom view

Figure 4.3: The platform prototype. Each letter denotes a different component:

A = Reflection receiver
B = Wires to the photodiodes
C = LED controller
D = Communication bridge between shine and the PC
E = LED driver
F = The LED
G = Wires to the analyser and power supply
H = Three photodiodes

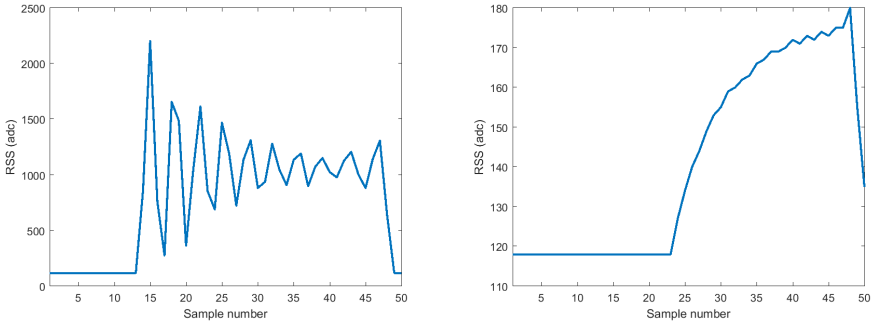

(a) Unfiltered flash

(b) Filtered flash

Figure 4.4: Two flashes captured with the platform. Left is unfiltered, right is filtered.

Chapter 5

Flash Analysis

The goal of this chapter is to find a method, capable of obtaining consistent measures of the environment from measured flashes. Secondary goals are to achieve this with the shortest flash and while using a small amount of computation power.

In this chapter, the platform is set-up as seen in figure 5.1. D in the Figure represents the distance between the device and the reflecting surface (the wall in this case). All measurements presented in this chapter have been made in a darkroom, a room where no lights from outside can enter, so the test result won't get influenced by other illumination sources.

The set-up will first be used to get a reasonable understanding of what flashes look like and how settings of the flash generator influence the received flash. Then, several methods for obtaining a measure of the environment from flashes will be presented and compared. This chapter will conclude with the final settings used in the flash generator and an algorithm to obtain a consistent measure of the environment from the received flash.

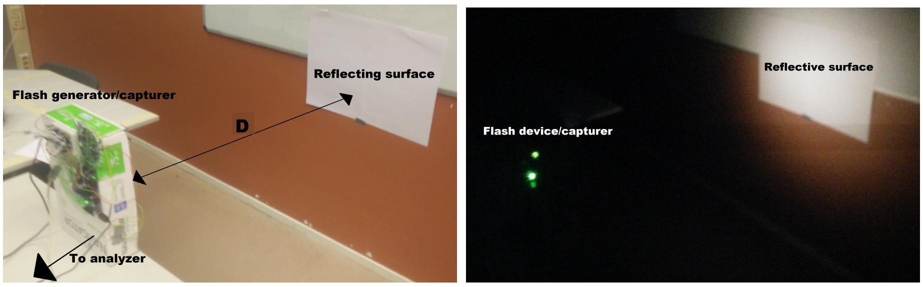

(a) Test setup in illuminated environment (b) Test set-up in dark environment

Figure 5.1: Test set-up used to capture flashes in the darkroom.

5.1 Flash properties

The test set-up has several parameters which can affect the perceived flash: T_{on} (on time of the LED), I (brightness of the LED), S_{PD} (sensitivity of the photodiode) and D (distance between device and reflecting surface). This section shows how each of these parameters influences the received signal. Note that the period, T, is not present in the list as should not influence an individual flash as long as the flashes are not too close together.

Figure 5.2(a) shows several responses for different T_{on}. The Figure shows that all signals closely match each other, until the light is turned off. This is a useful property as this means it's possible to reduce the T_{on} with no influence on the signal, if the ending of the flash is not used.

Figure 5.2(b) shows the influence of using the different amplification circuits of the flash generator. It can be seen that the LED powered with more current (because of the smaller resistor) is perceived as brighter to the system than the lights powered with a smaller current. It's also observed that the LED powered with higher currents show up earlier to the system. This is because LEDs driven with higher currents turn on faster [7]. This means that if a lower LED current is used, a longer T_{on} is required to obtain useful information.

Figure 5.2(c) shows a set of measured flashes at a variety of distances from the wall. It clearly shows that if the distance increases, the observed light decreases. This is logical, as when light travels longer distances, the relative intensity of the light decreases.

Figure 5.2(d) shows what happens when the different photodiodes are used. As expected, the RSS rises once we increase the gain on the photodiode. S_{PD_3} almost instantly saturates as the gain is too strong when used in combination with I_1. S_{PD_3} is therefore also displayed with in combination with I_3. Another noticeable change is the frequency of the ripple, caused by the amplifier. This change is expected, as the resistor in the feedback loop of the amplifier was changed.

5.2 Flash features

This section explores what kind of features can be extracted from a flash signal. It will then compare the methods based on required T_{on}, precision, detectability and computational complexity.

5.2.1 Feature considerations

The maximum of a flash response could contain useful information. Even though the light at the first maximum has not fully turned on yet, it still is some measure of the perceived light. This can be especially useful if the maximum of the flash always occurs at the exact same moment in time

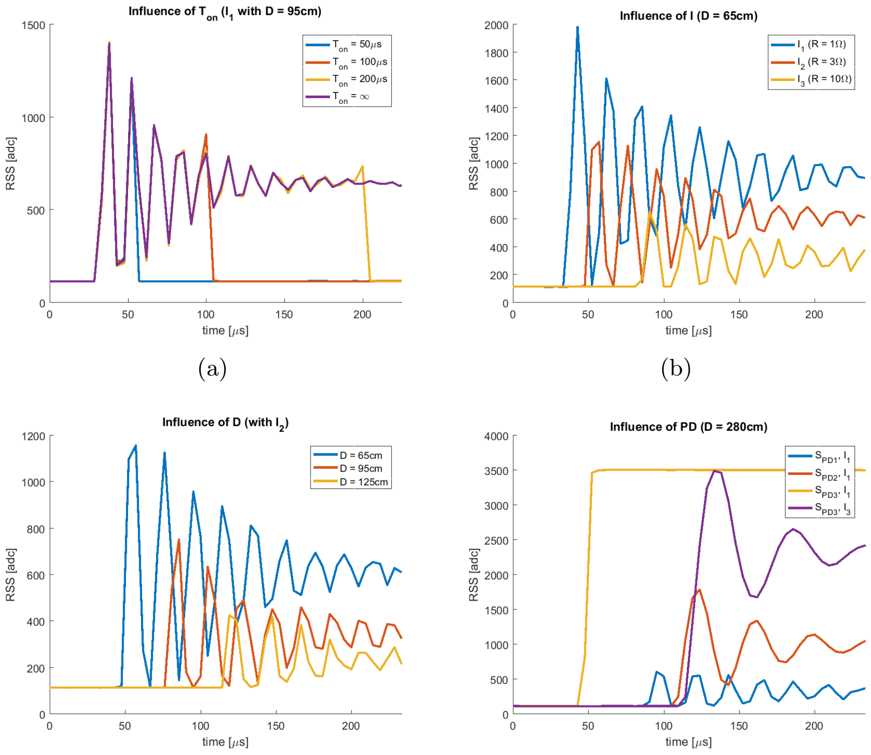

(a)

(b)

(c)

(d)

Figure 5.2: Several perceived flashes generated with different settings of T_{on}, I_{LED}, D and S_{PD}.

relative to the light turning on. If that's the case, then the maximum value of the first peak could provide us with enough information of the environment. If the maximum value of the first peak holds enough information, then a very small T_{on} can be used to obtain this value, as decreasing T_{on} does not significantly influence the height and form of the first peak.

Another possibility is to remove the oscillation of the signal with a low pass filter and then take the maximum value of the filtered signal. This method is less reliant on precise timing of the pulse. It also uses more samples of the signal and should therefore be able to obtain a value which better represents the reflections of the current environment than the maximum method. A downside to this method is that a filter designed to deal with one frequency of ripple, is not immediately suited to deal with the ripple frequencies of the other amplifiers

Another method considered is to use the area underneath the flash. This method has the advantage of being both simple and flexible. It does not matter if T_{on} is chosen big or small, it will always give a reliable result if T_{on} is not changed. It also does not care about the ripple frequency of the amplifier. This method simply sums all information available to obtain a measure of the reflections.

The final possibility considered is the filtered sum method. It first uses a filter to smooth the signal to then calculate the surface underneath it. It also requires multiple filters to be designed (one for each S_{PD} amplifier). It might however give a more detailed result than the filter method, as more information is used obtaining the data point.

5.2.2 Feature comparison

A test was created to compare the effectiveness of each feature with various settings in a full scale environment ($D = 280cm$). All of the features where extracted by the flash receiver simultaneously from consecutive flashes. The test was executed as follows:

1. Set the parameters for the given test (S_{PD}, I, T_{on}).
2. Move a highly reflective piece of cloth underneath the set-up at $185cm$ ($D = 95cm$).
3. Move the piece of cloth underneath the set-up again, but now from the other direction.
4. Calculate the *detectability* Q, of the received signal.

If we refer to the *'detectability'* in this thesis we mean Q as defined in equation 5.2. This equation calculates ratio between the standard deviation of the signal when nothing is passing by and the absolute minimum and maximum of when something is. The higher Q, the easier the signal should be to distinguishable from noise.

	Q: S_{PD_2}, I_1			Q: S_{PD_3}, I_3		
T_{on}	$150\mu s$	$200\mu s$	$250\mu s$	$150\mu s$	$20\mu s$	$25\mu s$
Maximum	35	38	40	5	5	5
Filtered maximum	39	65	66	20	27	33
Sum	45	75	95	18	20	26
Filtered sum	50	105	100	19	20	24

Table 5.1: Overview of the test results.

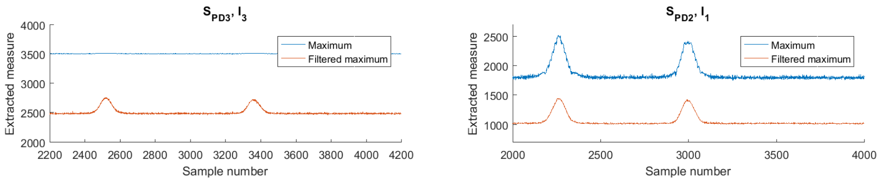

(a)

(b)

Figure 5.3: Data extracted from consecutive flashes using the maximum and filtered maximum methods with $T_{on} = 250\mu s$.

$$Q(PD) = \left(\frac{\mu(PD_{NoEvent}) - min(PD_{event})}{\sigma(PD_{NoEvent})} + \frac{max(PD_{event}) - \mu(PD_{NoEvent})}{\sigma(PD_{NoEvent})} \right) \tag{5.1}$$

$$Q(PD) = \frac{max(PD_{Event}) - min(PD_{Event})}{\sigma(PD_{NoEvent})} \tag{5.2}$$

The test was done with all combinations of S_{PD} and I. Only the combinations of SPD_2, I_1 and S_{PD_3}, I_3 gave potential usable results at full scale as for other combinations the flash was invisible or too bright (saturation) to observe. Several consecutive captured features can be seen in the Figures 5.3 and 5.4. These where then used to calculated Q for each scenario. An overview of all detectability values can be seen in table 5.1.

Based on the results of the Q test it was chosen to use the Filtered sum method with $T_{on} = 200\mu s$. This method gives better results than the maximum and filtered maximum methods because more measurements are used to determine the final value, leading to lower standard error. The reason that this method works better than the sum method lies in the fact that the filtered signal is a better representation for the environment that the rippled signal. This can also be seen in the difference between the maximum and filtered maximum.

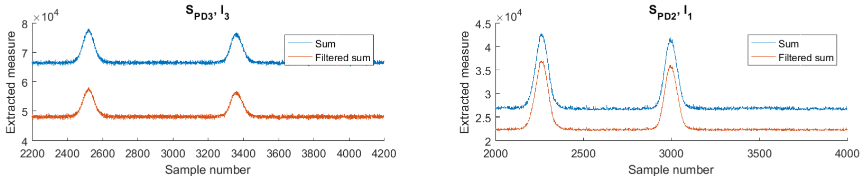

(a) (b)

Figure 5.4: Data extracted from consecutive flashes using the sum and filtered sum method with $T_{on} = 200\mu s$.

5.3 Flash period

The final parameter to decide is the period of the signal, T. This value has no influence on the detectability of the signal. It has however a clear influence on how much light is used by the system, as decreasing T directly increases the amount of flashes which occur. We can't choose a too low value for T as then users will observe the flickering of the light. Another reason T can't be chosen too low is that certain kind of noise still needs to be filtered out of the system. It is almost guaranteed that some 50Hz component will be seen in the signal, as long as it's connected to the net.

For these reasons, T was chosen to be $800\mu s$ resulting in a flash frequency of 125Hz. This frequency is high enough to filter the expected 50Hz noise. Even though literature recommends at least 200Hz to prevent the visibility of flickering, none was observed by 10 different test subjects with this setting of T.

5.4 Conclusion

In this chapter, several methods of extracting useful data from a flashes where presented. The Flash analyser will run at a frequency of 125Hz, a T_{on} of $200\mu s$ with maximum light intensity I_1 using the filtered sum method with S_{PD_2} to extract information from the reflections. These settings provide the best found detectability with the given platform. The next step for the project is creating an algorithm to analyse set of consecutive flashes.

Chapter 6

Analyser

The flash receiver now outputs values at 125Hz, which is a mixture of various light and noise sources. The next step is to create a real-time binary classification algorithm to convert the incoming samples into a logical value: Activity detected, or no activity detected. The detection algorithm should be designed with certain goals in mind:

- **High true positive ratio** - The system does not fulfil it's purpose if it is unable to reliably detect bypassing objects.
- **Low false positive ratio** - The system is useless if it classifies everything as activity. This would result in the light being on all the time and therefore, no energy being saved.
- **Fast response time** - If the algorithm manages to detect every bypassing person correctly, but it only triggers a detection when the object has already passed the light, then the system does not fulfil its purpose.
- **Low computational complexity** - If the algorithm uses too many calculations per incoming sample, the system would require a strong processor to analyse all incoming data. This makes the system expensive, if it where to eventually get implemented in the real world.

This chapter is separated in three parts. The first part shows what signals are received by the photodiode. The second part explains what methods considered to remove unwanted signals from the signal. The final part of this chapter shows what considerations where made to determine threshold of the binary classifier.

6.1 Received signals

In an ideal world, the dark sensing system only perceives light it emits itself, reflected by the environment. Figure 6.1 shows that this is clearly not the case. Several other factors are influencing the measurements. Equation

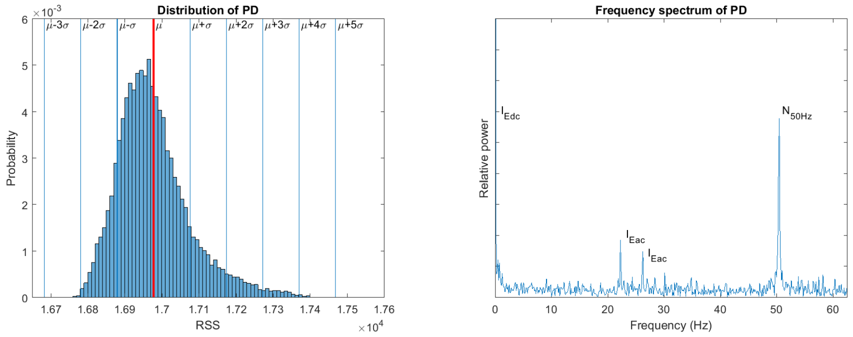

(a)

(b)

Figure 6.1: Properties of the obtained signal with the the filtered sum method.

6.1 has been devised and contains the most common signals the photodiode, PD, might receive. Each term of the equation will be discussed briefly while pointing out what the signal looks like.

$$PD = I_L\alpha + \sum_{i=1}^{n} I_{Edc_n}\beta_n + \sum_{i=1}^{n} I_{Eac_n}\gamma_n + N_{50Hz} + N(\mu, \sigma^2) \tag{6.1}$$

I_L represents the light emitted by the our luminaire. This gets multiplied with α, which represents the environment from the point of view of the system. These two terms represents the ideal response. The expected frequency of α should lie between $0.1Hz$ and $2Hz$ for by passing pedestrians and cars, as shown in chapter 3. The goal of the complete algorithm is to isolate α and detect significant changes in it real-time.

The next term, $\sum_{i=1}^{n} I_{Edc_n}$, represents all constant, but slowly changing light sources in the area. An example of this is moonlight. Moonlight illuminates the surrounding area, but slowly changes over time because moon moves relative to the system, or clouds block the moonlight which would otherwise be received by the photodiode. β_n represents the environment from the point of view of the moon.

$\sum_{i=1}^{n} I_{Eac_n}$ represents all fluctuating light sources in the area. Most lights connected to the power grid fall into this category. They typically turn on and off at 100Hz in Europe. Some of the light produced by these sources could reflect off of the environment γ_n and reach the system and therefore influence the received signal.

Another term in the equation is N_{50Hz}, which represents 50Hz noise from the powergrid. As long as the system is connected to the grid, some 50Hz components will be seen in the system. Especially if received signals are amplified 1000 times.

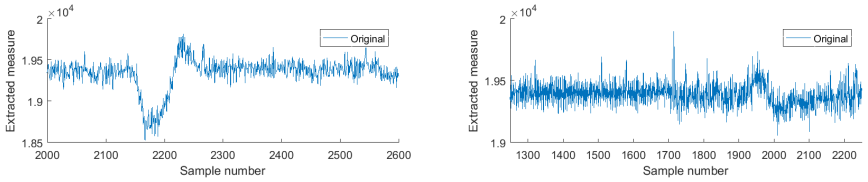

(a) (b)

Figure 6.2: Two signals of a person walking underneath the set-up. Figure (a) shows an optimistic case with an Q of 14.9 and (b) shows a harder scenario with an Q of 10.5.

The final term, $N(\mu, \sigma^2)$, represents the noise on the measurements not created by the ”predictable” sources listed above. This noise originates from the imperfections of the platform and electromagnetic noise in the environment. The exact distribution of the noise is unknown, but its likely to approximate a Gaussian curve. It is therefore represented by its mean (μ) and variance (σ^2) in the equation.

6.2 Filter methods

The goal of the filters is to get rid of unwanted signals in order to make the detection of α easier. Several digital filter types have been considered, each with different goals mind. The effectiveness (or failure) of each proposed filter will be shown where possible, with the help of the signals shown in figure 6.2. (a) shows an optimistic case with an original Q of 18.5. (b) shows a harder case with an original Q of 10.5 and a big spike at 1700, which is not part of the signal. This figure will display the filter working in a much harsher condition.

6.2.1 Low-pass filters

A low-pass filter can be used to remove I_{Eac_n} and N_{50Hz} from the measured signal as their frequencies are far removed from the signal we are interested in α (0.1Hz - 2Hz). Low-pass filters have one big downside for the system. They introduce a delay in the signal, which is bad for the overall response time. Several filters have been tested. The final result is shown in figure 6.3 and is a second order IIR low-pass with its corner frequency at $5Hz$. Using this filter, the complete N_{50Hz} component of the signal is removed and in most cases, I_{Eac_n} is removed as well. We are however unable to guarantee the removal of I_{Eac_n} because of possible signal aliasing.

Signal aliasing is a phenomenon which occurs if the sample rate F_s of a system is too low compared to the signal being sampled. If F_s is smaller then twice the frequency of the sampled signal, the signal will appear as

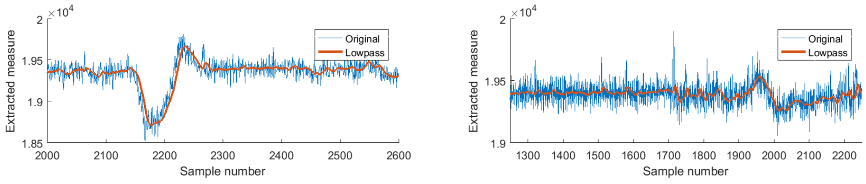

(a) (b)

Figure 6.3: A low-pass filter ($F_{cutoff} = 5Hz$) applied to the two example signals used to remove I_{50Hz} and I_{Eac}. The Q for signal (a) increased to 27.9 from 14.9 and the Q of signal (b) increased to 11.7 from 10.5.

another frequency instead, an alias. This frequency is called F_{alias} and can be calculated with equation 6.2, where n is the closest integer multiple of F_s to the signal being aliased (F_{Iac}).

$$F_{alias} = |F_s * n - F_{Iac}| \tag{6.2}$$

Almost all lights have a flicker frequency higher than half the sample rate of the system and will therefore alias. In Europe most lights have blink frequencies which are multiples of $100z$ or $200Hz$ (2 or 4 times the frequency of the power grid) and will therefore show up with alias frequencies of $25Hz$ and $50Hz$. These frequencies can still be removed with the used low-pass filter. There is however no grantee that all lights will blink at a multiple of $50Hz$. In the Americas for example the grid is powered at $60Hz$. The chance is very high that a light in the U.S. typically flickers at $120Hz$, which will alias at $5Hz$. This frequency is too low for the low-pass filter to remove and will have to be dealt with in another way (if it occurs).

6.2.2 High-pass filters

High-pass filters can be used to remove I_{Edc_n} from the signal. In this specific case, that's very hard as the frequency we are interested in is very close to 0. It works, but it takes the filter a long time to settle if the F_{Cutoff} is chosen too low. Several filters have been tested, and the final result applied to the two test signals is shown in figure 6.4.

6.2.3 Moving average filters

A moving average can be used to reduce $N(\mu, \sigma^2)$ and the remaining F_{allias}. A moving average is effectively a simple low-pass filter with specific frequencies being removed completely at $\frac{F_s}{n} * x$, where n is the number of samples in the moving average and x any integer greater than 0. Therefore, a makeshift filter can be created instantly if F_{alias} is known, with $n = \left|\frac{F_s}{F_{alias}}\right|$.

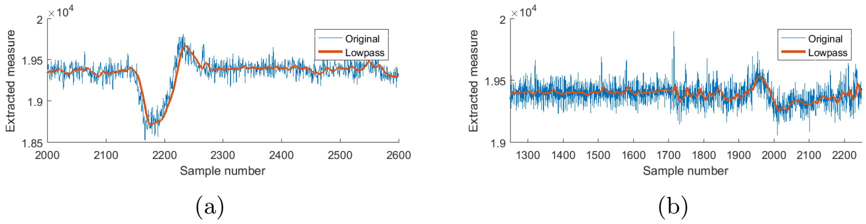

Figure 6.4: A high-pass filter ($F_{cutoff} = 0.01Hz$) applied to the two example signals used to remove I_{Edc} from the signal. The Q for signal (a) increased to 30.9 from 27.9 and the Q of signal (b) increased to 13.3 from 11.7.

F_{alias} could be determined with the help of a Fourier transformation and then filtered away with a makeshift moving average. Yes, the Fourier transform costs a lot of computation power which is against our goal of creating a computationally light algorithm, but the transform wouldn't have to be ran every sample. It is probably good enough to run it once every 10 minutes to check if F_{alias} is detected and/or has changed.

Another advantage the moving average brings is that it reduces the noise by a factor $\sqrt{(n)}$, where n is the number of samples in the moving average. It was therefore considered to scale the moving average, based on the current standard deviation of the noise with the help of equation 6.3. The presented formula calculates n, so that the expected noise level ($T \cdot \sigma$) is always smaller after the moving average than the expected signal ($\mu \cdot ss$).

This method has two downsides. The first is that a moving average, capable of changing every incoming sample is computational expensive. If n changes, then the full moving average needs to be re-evaluated (n summations, 1 division)) instead of using a simple update rule (1 summation, 1 division). Another downside is that if n gets too large, the response time of the system goes down. For these two reasons, the scaling moving average was not implemented in the final algorithm.

$$\frac{signal}{noise} = 1 = \frac{\mu \cdot ss}{T \cdot \frac{\sigma}{\sqrt{n}}} \Rightarrow n = \left(\frac{T \cdot \sigma}{\mu \cdot ss}\right)^2 \tag{6.3}$$

6.2.4 Differential filter

The differential filter makes use of the fact that the system is not only able to sample when the light is turned on. Instead, it is possible to take samples while the light is turned off, to obtain PD_{dark}. This signal represents all the signals in the environment we are not interested in. If this signal is obtained very close to in time relative to PD ($20\mu s$), then we can assume that all fluctuating sources in both, PD and PD_{dark}, are equal. It's therefore

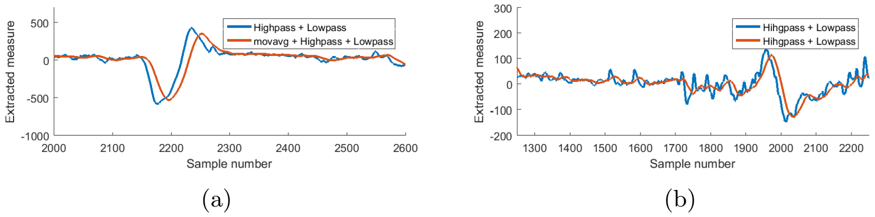

Figure 6.5: A 28 tabs moving average applied to the two filtered example signals used to remove the remaining $4.5Hz$ component of the signal. The Q for signal (a) increased to 35.6 from 30.9 and the Q of signal (b) decreased slightly from 16.6 to 13.3.

possible to subtract the two signals, which would result in the filtered signal shown in equation 6.5.

$$PD_{dark} = \sum_{i=1}^{n} I_{Edc_n}\beta_n + \sum_{i=1}^{n} I_{Eac_n}\gamma_n + N_{50Hz} + N(\mu, \sigma^2_{dark}) \tag{6.4}$$

$$PD - PD_{dark} = I_L\alpha + N(0, \sigma^2 + \sigma^2_{dark}) \tag{6.5}$$

There are several downsides to this filtering method. The first is that we are subtracting two separate measures of the same noise signal. This leads to a higher variance on the complete signal and therefore a higher noise level. Another downside of this method is that it does not work properly with the current hardware set-up because the PD_{dark}, on its own, is below the sensitivity threshold of the receiver and is therefore unmeasurable, unless there is a lot of stray light in the area.

6.2.5 Filter overview

Several methods for removing unwanted parts of the received signal have been presented and summarised in table 6.1 and result in a better Q. The final solution implements the low-pass, high-pass and moving average with scaling based on F_{alias}. Figure 6.6 shows the remaining distribution of the noise on the signal.

6.3 Detection threshold

The next step in creating the binary classification algorithm is to determine classifying thresholds or rules. If an extracted value of the set of samples crosses the threshold, then the set gets classified as activity detected. A naive solution to the threshold problem would be to sample a fixed amount

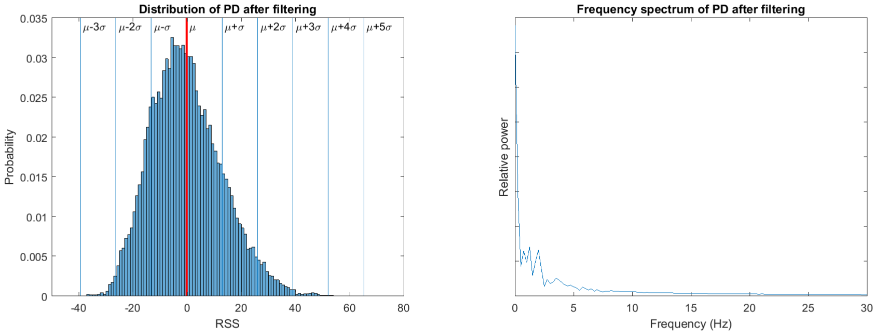

(a) (b)

Figure 6.6: Properties of the signal after filtering. Note that (b) is zoomed in on the frequency axis compared to Figure 6.1(b)

.

Filter type	Goal	Notes	In final algorithm?
Low pass filter	Filter I_{Eac} and N_{50Hz}	Can't guarantee the removal of I_{Eac} due to signal aliassing	Yes
High pass filter	Filter I_{Edc}	Takes a long time to settle if a step is received	Yes
FFT based moving average	Filter F_{alias} and reduce $N(\mu, \sigma)$	Works, as long as F_{alias} is not too close to $I_L \alpha$	Yes
SNR based moving average	reduce $N(\mu, \sigma)$	Worked, but introduced huge delays for high σ and was is computational intensive	No
$PD - PD_{dark}$	Filter I_{Eac}, N_{50Hz} and I_{Edc}	Only worked in illuminated environments which made it unreliable to filter N_{50Hz}	No

Table 6.1: Overview of the filter methods described in this section.

of values when there are no objects in sight. Then, take the maximum and minimum of the sampled values and if the signal ever moves out of the range of the found values, activity is detected. Even though this might work consistently in a dark room (lab environment with no lights), it fails to work in a more realistic environment. If a "dirty" device in the environment turns on then this could increase the noise level in the environment. which would lead to false detections.

This failed method shows that the threshold needs to be able to adaptable based on the noise in the environment. Two other algorithms have been considered, which are possibly capable of adjusting their thresholds in an intelligent manner.

6.3.1 Standard deviation based threshold

The first method is based upon the standard deviation. We could set the detection threshold based on the current measure on σ. Several real-time algorithms are known to calculate rolling σ, the standard deviation over all samples which have passed by. This measure gives a good estimate of the noise in the environment until something happens. for example, an object passes by, an "extreme" change in the signal will occur and the rolling standard deviation will be deluded with non-noise samples, ruining the noise estimate.

This issue can be solved by using a moving standard deviation. This method only uses the most recent m samples to obtain σ and bases it's detection threshold on this value. This means, that if an event occurs, the algorithm only remembers it for m samples. By using a system with only a short-term memory, we can create a flexible system which automatically adjust to permanent changes in the environment.

Using the idea of moving σ, we can create a simple threshold algorithm with equation 6.6. This equation calculates the z-score for the most recent sample out of the filter section $\overline{X}[i]$ and compares it with threshold value T. Then if z is greater than T or smaller than $-T$, it triggers a detection. σ_i and μ_i in this equation represent the moving mean and standard deviation over the most recent m samples at i.

$$z_i = \frac{\overline{X}_i - \mu_i}{\sigma_i} \qquad (-T < z_i < T) \rightarrow detection \tag{6.6}$$

Figure 6.7(a) shows the described algorithm in action. It can be seen that the bypassing person is detected at sample 2962. This is a good result, but rather slow, especially since we are able to see the signal rise from sample 2875. The reason why the algorithm does not trigger a detection is because the threshold ($T * \sigma$, the red line in figure 6.7(a)) has risen slightly due to the variance on being increased, which is caused by change in the signal itself. This problem can be solved in a very simple way. Prevent σ from

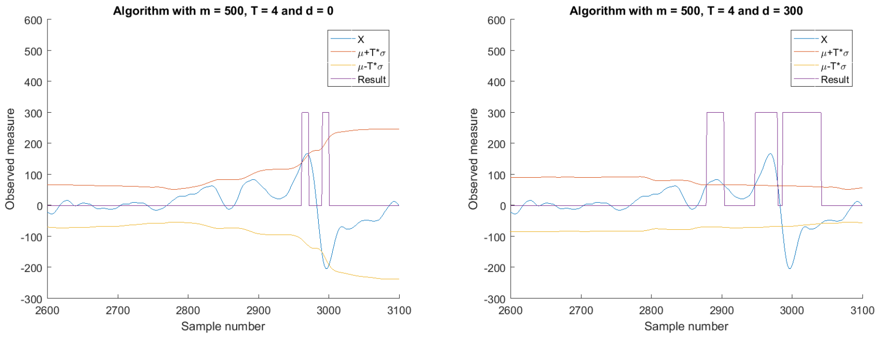

(a)

(b)

Figure 6.7: Working of the algorithm visualized with and without delay (d) between the standard deviation (σ) and the signal (X).

being updated before an event happens. This can be achieved by adding a small delay of d samples between X and the threshold. An example of this is shown in Figure 6.7(b), where the event is detected at 2879 samples, which is 83 samples (0.66 seconds) earlier than the previous result.

Several other parameters where added to further improve the classification algorithm. The first one is to add a linear offset $k \cdot \sigma$ to the detection threshold, because the noise distribution of the device is not balanced, meaning that there are more outliers on one side of the mean, than there are on the other side. This can be seen in Figure 6.6(a). If we where to move μ slightly more to the right with a factor 0.75σ, then the distribution would be more balanced (all samples lie between $\pm 3.5\sigma$) which results in a better overall sensitivity.

Another improvement we can make is to not look at only one observation of $\overline{X}$, but L consecutive ones instead. If we then only trigger a detection if l out of L samples cross the threshold then it might be possible to run the algorithm with a smaller T and therefore detect more events.

Equation 6.7 shows a mathematical representation of the threshold algorithm. A graphical overview of the complete algorithm (including the filter section) can be seen in Figure 6.8.

$$\sum_{i=-L}^{0} \left\lfloor \frac{\overline{X}_i + k \cdot \sigma_{i-d} - \mu_{i-d}}{T \cdot \sigma_{i-d}} \right\rfloor \geq l \rightarrow detection \tag{6.7}$$

6.4 Conclusion

This chapter described the considerations made into designing an algorithm capable of classifying a set of consecutive flashes. The resulting algorithm

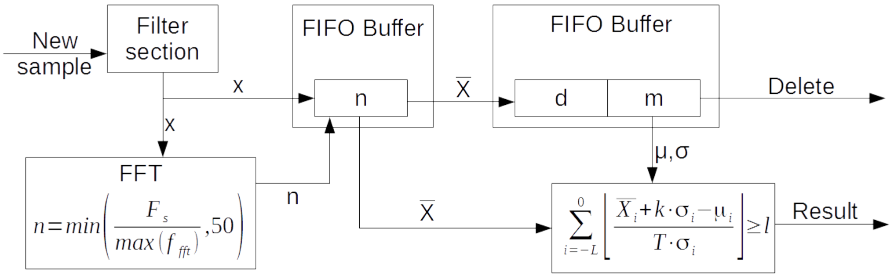
New sample
Filter section
FIFO Buffer
FIFO Buffer
x
x
n
$\overline{X}$
d
m
Delete
μ,σ
FFT
$n=min\left(\frac{F_s}{max(f_{fft})},50\right)$
n
$\overline{X}$
$\sum_{i=-L}^{0}\left\lfloor\frac{\overline{X}_i+k\cdot\sigma_i-\mu_i}{T\cdot\sigma_i}\right\rfloor\geq l$
Result

Figure 6.8: Graphical overview of the presented algorithm.

(seen in Figure 6.8) feature two sections. A filter section and a threshold section.

The filter section is used to remove the uninteresting signals from the consecutive flashes to improve the detectability of the signal. The best results where archived by using a low-pass filter (5Hz), a high-pass filter (0.1Hz) and a moving average (based on the biggest noise frequency still left in the signal). The threshold section is used to classify the remaining signal into two groups: Activity detected and no activity detected. This algorithm however requires several parameters to work. These parameters will be determined in the next chapter.

Chapter 7

System evaluation

In the previous chapter an algorithm has been proposed, which should be capable of classifying a set of consecutive samples into two groups: Activity detected or no activity detected. The algorithm is however dependent on several parameters which have not been determined yet. The goal of this chapter is to find a set of parameters for the algorithm and evaluate the system using the algorithm tuned with those parameters.

This chapter starts with showing the test set-up which will be used to create a diverse dataset. This dataset will then be used to find parameters for the algorithm with which we evaluate the system. This chapter finishes with evaluating the performance of the system.

7.1 Test set-up

The test set-up used for evaluating and tuning the system can be seen in Figure 7.1(a). It shows the platform placed at 280cm above the ground in a room at night. Figure 7.2 shows 15 seconds of received samples when the system was turned on. It can be seen that all described noise sources in section 6.1 where detected in the test environment.

Figure 7.1(a) also shows three possible paths a pedestrian can walk. Path 1, the centre path, is placed directly under the light. Path 2 and 3 where placed at 30cm and 60cm from the centre path. The pedestrian was asked to wear one of the hoodies shown in Figure 7.1(b) before traversing one of the paths. The different colours where used to ensure that the system was tested on various albedo's.

The ground where the pedestrian walked upon also varied. It was either a lacquered wooden floor or a blue carpet. The carpet on the floor produced a mostly diffuse reflection. The wooden floor produced a diffuse and spread reflection. These two floors were chosen to simulate how the system performs in different environments.

With the described set-up we created test-cases in the following manner:

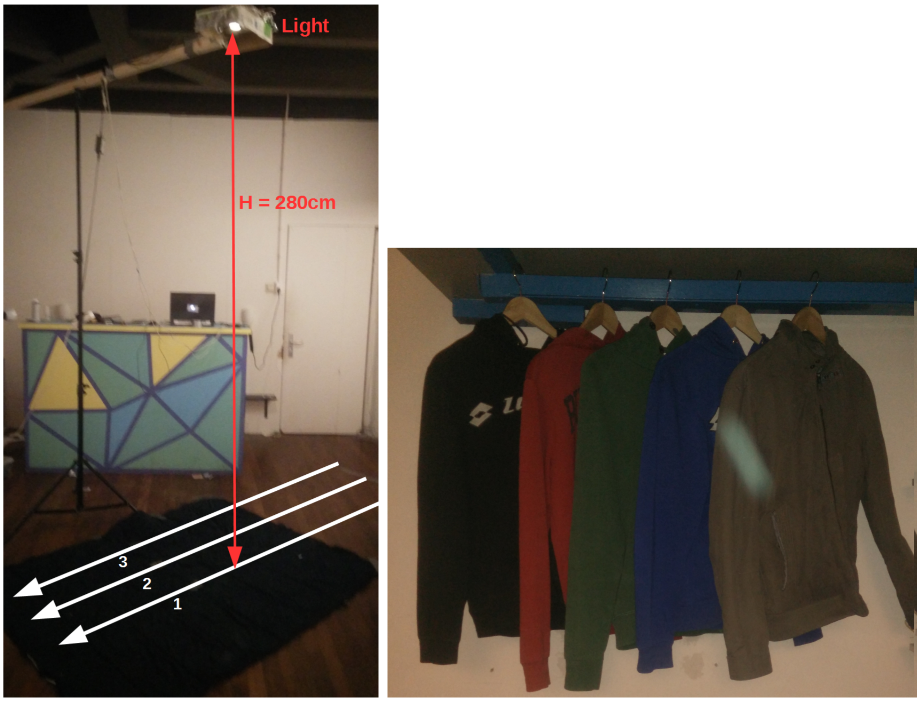

(a) (b)

Figure 7.1: (a) shows a picture of the test set-up with the blue carpet. The white arrows on the floor represent the three different paths the test subject walked over. The light is placed at a height of 2.8m. (b) shows the different clothing worn during the experiment (black, red, green, blue and grey).

1. Position a person at the beginning of a path.
2. Start the gathering of samples and let the person wait for ± 35 seconds.
3. After ± 35 seconds, the person starts walking
4. When the person has reached the end of a path, stop the measurement.

This procedure was repeated six times for each combination of floor material, path and hoodie colour, resulting in 180 unique test-cases. An example test-case can be seen in Figure 7.3.

A test-case is split up in three sections. The first section (the first 25 seconds of data) serves to initialise the filters of the filter section and to fill the FIFO buffers used to calculate the moving σ and moving μ. After these 25 seconds the system can start detecting events. This is where section two starts. In this section, no events which should be detected by the algorithm are present. Then, after 10 to 15 seconds, section three begins when the person starts walking. In this section, the algorithm should trigger a detection.

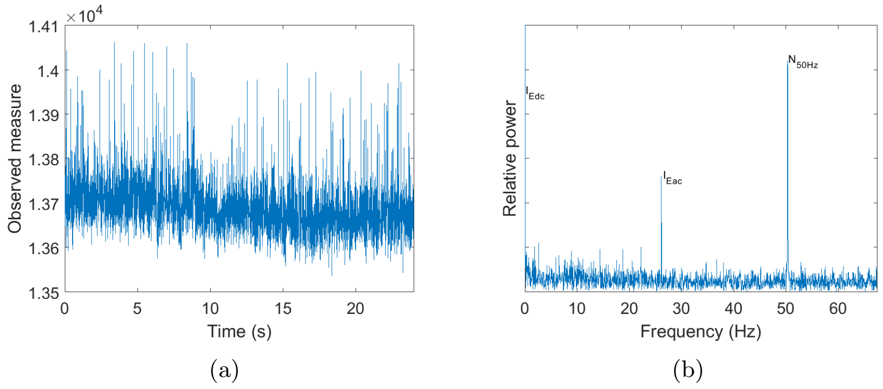

Figure 7.2: (a) shows the received signal and (b) shows the frequency of this signal. I_{Eac} and N_{50Hz} are best seen in figure (b). I_{Edc} is best observed in (a) (the slowly dropping signal).

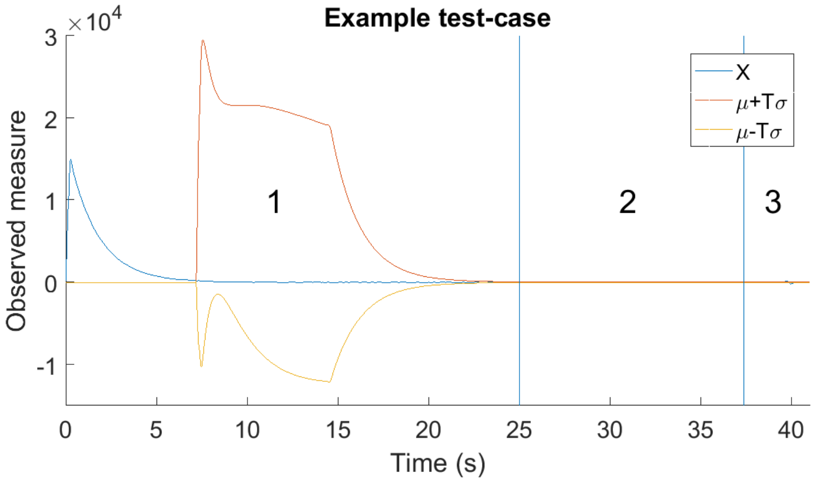

Figure 7.3: An example scenario with the tree sections marked. The first section is used to initialise the filters, moving mean and moving standard deviation. The second section is use to check for false positives. The first section is used to check if the event gets detected properly.

	d	m	l	L	T	k
Min	0	1	1	1	1	-1
Max	1000	1000	10	10	10	1

Table 7.1: Overview of the possible input genes for the genetic algorithm.

	d	m	l	L	T	k	Fitness
ALG_1	980	890	7	9	4.5	0.2	91%
ALG_2	860	980	8	10	5.9	-0.7	83%

Table 7.2: The settings found with the genetic algorithm. STD_1 was trained with dataset S_1 and STD_2 was trained with dataset S_2.

7.2 Algorithm parameters

A genetic algorithm (GA) was used to find parameters fo the algorithm. GA's are commonly used to generate high-quality solutions to optimization and search problems. In this case, we need to find good settings for the algorithm.

A GA needs two things to work. The first is a way to summarise a solution as a *gene*. In our case, a gene is simply a set of numbers which represent the parameters of the algorithm. The range of allowed inputs can be seen in Table 7.1.

The second thing a GA needs to work is a fitness function. This function evaluates the input gene and scores it based on its performance. In our case, we want a gene representing an algorithm, which detects persons passing by while not triggering when nobody passes by. This can be achieved by having the fitness function evaluate a dataset S and counting the amount of test-cases where it correctly and incorrectly detects the pedestrians. The final fitness can be calculated with equation 7.1, where TP is the amount of correct detections in the observed dataset, FP is the amount of false detections in the observed dataset and N represents the amount of test-cases in the dataset.

$$Fitness = \frac{TP - FP}{N} \cdot 100\% \tag{7.1}$$

The described fitness function was used to train two separate algorithms. The first algorithm ALG_1 was found using dataset S_1, which contained the 90 test-cases created with the wooden floor. The second algorithm trained, ALG_2, was found using dataset S_2, which contained the 90 test-cases created with the carpet. The found algorithms can be seen in Table 7.2.

	S_1			S_2			$S_1 \cup S_2$		
Algorithm	TP (%)	FP (%)	Fitness	TP (%)	FP (%)	Fitness	TP (%)	FP (%)	Fitness
ALG_1	86 (96%)	4 (4%)	91%	81 (90%)	11 (12%)	78%	167 (93%)	15 (8%)	84%
ALG_2	84 (93%)	3 (3%)	90%	81 (90%)	6 (7%)	83%	165 (91%)	9 (5%)	87%

Table 7.3: Results of testing the found algorithms against all datasets.

7.3 Evaluation

The two found algorithms where evaluated against three different datasets: S_1, S_2 and S_3. S_3, is the union of S_1 and S_2, and contains all 180 testcases. Results of this evaluation can be seen in Table 7.3. We are aware that evaluating the algorithm with the dataset it was trained with gives biased results, but they were added for the sake of completeness. The most interesting sections of the table are marked blue. These sections show the results of testing ALG_1 on S_2 and ALG_2 on S_1. It can be seen that both algorithms seem to perform reasonably well as they achieve a fitness of over 75%.

This method however, does not give a good representation of how the system performs in the real world, as the fitness score of an algorithm does not tell us how much energy is saved and how much of the bypassing persons are actually detected. A better way to gain insight in the performance of this system is with recall and the false positive ratio.

Recall, R, is defined in equation 7.2 and gives us insight in how often the system fails to detect an object passing by. $R = 1$ means that all events are detected were $R = 0$ means that none of the pedestrians are detected. The false positive ratio, FP_r, is defined in equation 7.2 and gives us insight in how often the system makes a false detection. Because it's known how much time we observe when we determine if a false positive occurs, we can calculate the chance on a false positive per minute with equation 7.3.

If we evaluate the algorithms with these metrics, we see that ALG_1 has a 18% chance on a false positive every minute and ALG_2 a 54% chance. These numbers show that the system, with the current algorithm settings, makes too much mistakes and won't be usable to save energy. It is however possible to manually adjust the found parameters to better suit our system.

$$Recall = R = \frac{TP}{TP + FN} \quad FP_r = \frac{FP}{FP + TN} \tag{7.2}$$

$$P_{FP/minute} = 1 - \left(1 - \frac{FP}{FP + TN}\right)^{6t} \tag{7.3}$$

The easiest way to manually adjust the algorithm is by changing the value of T. T directly influences the detection threshold. Raising T will by definition, decrease the amount of false positives (lowering FP_r) and true

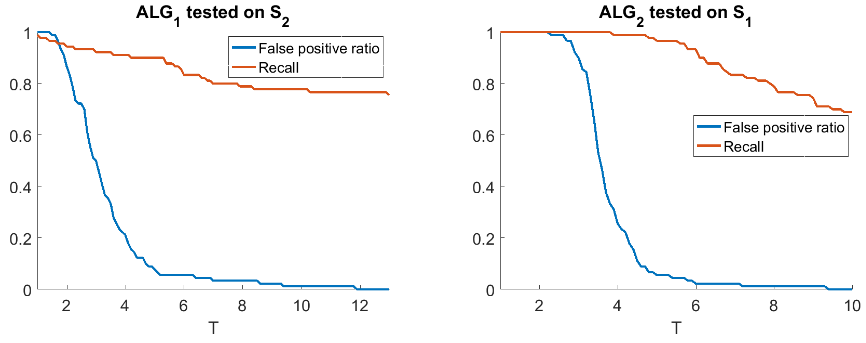

(a) (b)

Figure 7.4: The false positive ratio and recall plotted as a function of T, for both created algorithms.

positives (lowering recall) we detect. Two plots, showing R and FP_r as a function of T for both algorithms can be seen in Figure 7.4.

In these plots it can be seen FP_r drops fairly fast if T increases, until FP_r reaches 0.1. From this point, T needs to increase a lot, to further increase FP_r significantly. This is because the false positives in these test-cases are not caused by the previously described noise sources but by artefacts occurring in the test data. One of such artefacts is shown in Figure 7.5(a) at $t = 32s$.

These artefacts are caused by slight fluctuations in the power supply of the flash receiver. This part of the system is powered by an USB port of the analyser. Slight voltage drops in the USB ports are common but usually no problem as the changes are minimal. If they get amplified 5600 times however, they become visible and will influence the measurements of the photodiode. this problem could be solved by powering the system with a battery or a very stable power supply. This is however no longer possible for this project due to time constraints.

It is however still possible to ignore the artefacts by choosing an ideal value for T with the help of Figure 7.4. For example, if we want a system which does not trigger any false positives (e.g. $FP_r = 0$), then we have to choose $T = 12$ for ALG_1 and $T = 9.6$ for ALG_2. This leads to the detection results shown in Table 7.4. It can be seen that the detection ratio of persons walking directly under the light is good (90% and 100%), but the further we move away from the centre, the worse the detection ratio (recall) becomes.

The amount of detections can be increased by lowering T, but this leads to more false classifications by the system. For example, if we allow a false positive ratio of 0.05 (26% chance on a false positive every minute), we can greatly increase the amount of true detections. This can be seen in Table 7.5. If we look at the results by colour in this table, we can see that the system

	$ALG_2(S_1) \rightarrow FP_r = 0$			$ALG_1(S_2) \rightarrow FP_r = 0$		
	R Lane 1	R Lane 2	R Lane 3	R Lane 1	R Lane 2	R Lane 3
Red	1	1	1	1	0.5	0.83
Black	1	0.33	0	1	0.5	0
Green	1	0.83	0.67	1	0.83	0.83
Blue	1	0.83	0	1	0.83	0.17
Grey	0.5	1	0.5	1	1	1
Total:	0.9	0.8	0.43	1	0.73	0.57

Table 7.4: Overview of the performance of ALG_2 when tested on S_1 and ALG_1 on S_2 with T set so that $FP_r = 0$.

	$ALG_2(S_1) \rightarrow FP_r = 0.05$			$ALG_1(S_2) \rightarrow FP_r = 0.05$		
	R Lane 1	R Lane 2	R Lane 3	R Lane 1	R Lane 2	R Lane 3
Red	1	1	1	1	0.5	0.83
Black	1	0.83	0.67	1	0.83	0.17
Green	1	1	1	1	0.83	1
Blue	1	1	1	1	0.83	0.5
Grey	1	1	1	1	1	1
Total:	1	0.97	0.93	1	0.8	0.7

Table 7.5: Overview of performance of ALG_2 on S_1 and ALG_1 on S_2 with T set so that $FP_r = 0.05$.

has trouble detecting pedestrians wearing blue and black clothing. This makes sense. The black clothing does not reflect a lot of light compared to the other colours and is therefore less visible to the system. The low detection ratio of blue clothing can be explained with the help of Figure 7.5(b). This Figure shows the colour spectrum of the used LED. It can be seen that considerably less blue light is generated by the LED than the other tested colours. It therefore makes sense that the signals created with the blue hoodie are less visible to the system.

7.4 Conclusion

We have developed a method which is capable of analysing a set of consecutive flashes with the goal of detecting bypassing pedestrians, even when a considerable amount of noise sources are mixed in the signal. The created filters and algorithms managed to achieve a combined recall between 0.73 and 0.9 depending on the setting of T and the amount of allowed false positives ratio (0 to 0.05). The system has shown to work on two floors types and on several colours of clothing.

We are aware that the evaluation of the system is minimal, as the system

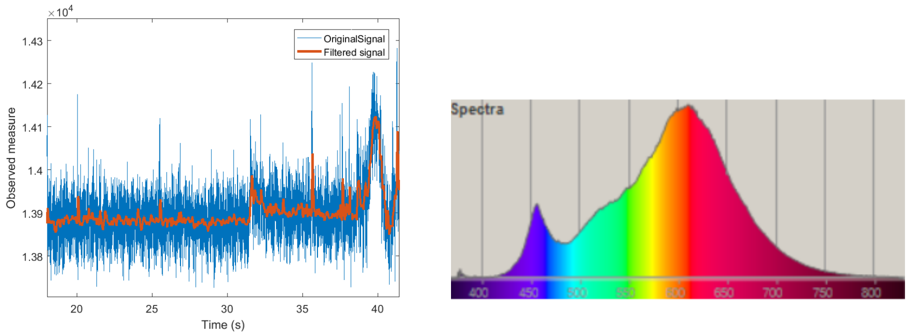

(a)

(b)

Figure 7.5: (a) shows an example of an artefact at $t = 32s$, caused by fluctuations in the power supply. (b) shows the frequency spectrum of the light emitted of the LED used by the system.

was with a limited dataset. The algorithm was then tweaked by adjusting T, to fit the data even more. This method of evaluation at least shows the potential of the system. It also manges to expose some key flaws. It has trouble detecting pedestrians wearing black and blue clothing and has regular false detections if we try to achieve a high detection ratio because of a flaw in the hardware design.

The most direct approach to deal with the identified problems is to improve the hardware design. Changing the LED with one, which emits light more evenly distributed along all wavelengths, will improve the detection ratio of bypassers wearing blue. Changing the power supply and implementing the full system with a detected processor will remove the artefacts and decrease the complexity of the project. It will also allow for the wires to the photodiodes to be shortened and therefore reducing the total amount of noise received by the system.

Chapter 8

Conclusions and Future Work

8.1 Conclusions

This thesis proposed a new method for activity detection while only using visible light and a photodiode with the goal of saving energy. This can be achieved by measuring reflections of light with a photodiode, produced by a light. Our model shows that the changes in reflection are measurable by a photodiode if a person walks by the system.

A flash does not appear as a perfect square to a photodiode. Therefore, a method was created to extract the most relevant features from a flash. These features were then analysed by a newly created algorithm capable of analysing consecutive flashes.

A prototype has been made with off-the-shelve parts, implementing the proposed system. The prototype was created to work in a hallway of a university. The prototype showed to detect between 73% and 90% of all bypassing pedestrians depending of what a false positive ratio was allowed (0 to 0.05).

Even though the prototype has a relatively high false positive ratio, it serves as a good proof of concept for detecting activity with short flashes of visible light. Most of the found flaws in the system can be solved by improving the hardware platform.

8.2 Future Work

The presented work serves as a proof of concept for detecting activity in the line of sight of an LED. I personally think that the potential of this system is huge, especially if a dedicated platform is created, as most shortcomings of the current prototype can be solved if a better platform is built. Below I have listed several ideas for future research.

- **Multiple units in one room** - The algorithm is currently designed for a stand-alone device. If we would hang multiple of these systems in the same room then it's likely that some of the light flashes overlap and trigger a false positives regularly. This problem could be solved by having each detector flash in another timeslot, but this requires more research.

- **Tracking** - The system is currently only detecting activity. It could also be expanded for other purposes. It might for example be possible to use multiple photo diodes, lenses or field of view blockers to track bypassing pedestrians.

- **A dark sensing network** - Multiple working units in one room is nice, but multiple units working together to track, predict and illuminate the path of a pedestrian is nicer. This could be achieved by having the devices communicate using the flashes already generated by the device (visible light communication).

Bibliography

[1] Marilyne Andersen. Types of reflection. https://www.flickr.com/photos/mitopencourseware/4815499473/.

[2] Arduino.cc. https://store.arduino.cc/arduino-uno-rev3.

[3] Lilian Tieman Chris van der Nat, Hans Schelvis. *Bestaande bouw, Handboek Politiekeurmerk Veilig Wonen.* Centrum voor Criminaliteitspreventie en Veiligheid, december 2015.

[4] Thiemo Voigt Carlos Perez-Penichet Elena Di Lascio, Ambuj Varshney. Localight - a battery-free passive localization system using visible light. *IPSN '16 Proceedings of the 15th International Conference on Information Processing in Sensor Networks*, (60), April 2016.

[5] A. Galvin and J.K. Guscott. Passive infrared detector. Google Patents, March 1982. US Patent 4,321,594.

[6] H. Akbari H. Taha, D. Sailor. High-albedo materials for reducing building cooling energy use. Technical report, Lawrence Berkeley Lab., CA (United States), January 1992.

[7] H. Halbritter. High-speed switching of ir-leds (part i) - background and datasheet definition. Technical report, OSRAM, Opto Semiconductors, March 2014.

[8] L. Klaver and M.A. Zuniga. Shine: A step towards distributed multi-hop visible light communication. *12th IEEE International Conference on Mobile Ad hoc and Sensor Systems (MASS)*, pages 235 – 243, October note = 2015.

[9] Ikea 702.880.22 led1336r4. http://lamptest.ru/review/ikea-70288022-led1336r4/.

[10] K. Iio M. Fukuda, H. Numakuraand and A. Hidaka. Human body detection system. Google Patents, March 1994. US Patent 5,369,269.

[11] S. Bissig M. Waelchli and T. Braun. Intensity-based object localization and tracking with wireless sensors. January 2006.

[12] Esmail M.A. and H.A. Photon Fathallah. Indoor visible light communication without line of sight: investigation and performance analysis. *Photonic Network Communications*, pages 159–166, October 2015.

[13] Mastech. *MS8229, Digital multimeter operation manual.*

[14] Jaakko Maentuasta Miika Valtonen and Jukka Vanhala. Tiletrack: Capacitive human tracking. *Pervasive Computing and Communications*, March 2009.

[15] Siddharth Rupavatharam Minitha Jawahar Marco Gruteser Richard Howard Mohamed Ibrahim, Viet Nguyen. Visible light based activity sensing using ceiling photosensors. *VLCS '16 Proceedings of the 3rd Workshop on Visible Light Communication Systems*, pages 43–48, October 2016.

[16] Ashok Agrawala Moustafa Youssef, Matthew Mah. Challenges: Device-free passive localization for wireless environments. *MobiCom '07 Proceedings of the 13th annual ACM international conference on Mobile computing and networking*, pages 222–229, January 2017.

[17] Marcos F. Guerra Medina Oswaldo Gonzlez and Inocencio R. Martn. *Advances in Optical Communication*, chapter Multi-User Visible Light Communications, pages 36–62. InTech, November 2014.

[18] L. Benini P. Zappi, E. Farella. Enhancing the spatial resolution of presence detection in a pir based wireless surveillance network. *Advanced Video and Signal Based Surveillance, 2007*, September 2007.

[19] Junwei Zhang. Passive localization with visible light. MSc thesis, TU Delft, 9 2016.

[20] Kevin Wright Zhao Tian and Xia Zhou. The darklight rises: Visible light communication in the dark. *MobiCom '16 Proceedings of the 22nd Annual International Conference on Mobile Computing and Networking*, pages 2–15, October 2016.

[21] Kevin Wright Zhao Tian and Xia Zhou. Lighting up the internet of things with darkvlc. *HotMobile '16 Proceedings of the 17th International Workshop on Mobile Computing Systems and Applications*, pages 33–38, February 2016.

[22] Zumtobel. The lighting handbook. In *You concise reference book*. Zumtobel, Schweizer Strasse 30, 6851 Dornbirn, AUSTRIA, 5th edition, 2017.

Appendix A

Code repository

This appendix is the github repository where all the raw data, code and MATLAB scripts can be found, used to create this thesis. It can be found at: `https://github.com/hkleingeld/DarkSensing`.

Appendix B

Flash analyser schematics

This appendix contains pictures of electronic schematic created for specifically the flash analyser. Schematics of the processor boards where not added, as only small changes small modifications (see section 4) where made to these boards. The original scematics can be found at:

- Flash analyser - `https://github.com/LennartKlaver/SDVN1`
- LED controller - `https://www.arduino.cc/en/uploads/Main/arduino-uno-schematic.pdf`

B.1 LED driver

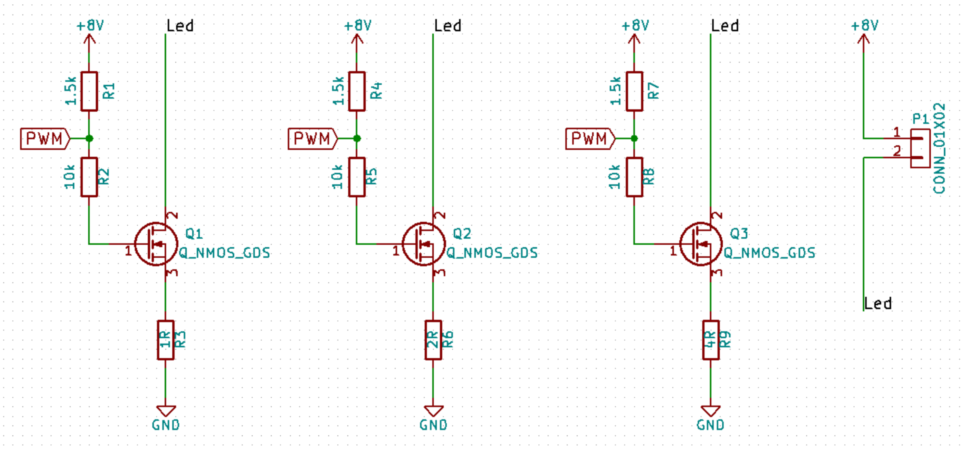

Figure B.1: Drivers used to drive the LED.